



## Review

# Engineering aerogel particles as next-generation drug delivery systems: a comprehensive review of recent advances



Susana M. Gomes<sup>a</sup>, Carlos Illanes-Bordomás<sup>a</sup>, Carlos A. García-González<sup>a,\*</sup>, Işık Sena Akgün<sup>b</sup>

<sup>a</sup> *AerogelsLab, I+D Farma Group (GI-1645), Department of Pharmacology, Pharmacy and Pharmaceutical Technology, Faculty of Pharmacy, iMATUS and Health Research Institute of Santiago de Compostela (IDIS), Universidade de Santiago de Compostela E-15782 Santiago de Compostela, Spain*

<sup>b</sup> *Department of Chemical and Biological Engineering, Koç University, Sarıyer, 34450 Istanbul, Turkey*

## ARTICLE INFO

## Keywords:

Aerogel particles  
Coating  
Biomedical applications  
Porous systems  
Controlled drug delivery

## ABSTRACT

Aerogels, defined as low-density solid materials with high porosities, open pore structures, and high specific surface areas, have shown increasing interest among the scientific and industrial communities. The engineering of aerogels in the form of spherical particles has been well documented for several applications and recent studies have highlighted the promising potential of use them as drug delivery systems. Therefore, this review article consolidates the recent progress on aerogel particle technology by providing a comprehensive and focused synthesis of the state-of-the-art of aerogel particle design specifically intended to enhance biocompatibility, stability, and targeted drug delivery. The engineering technologies herein presented, based on droplets production and on the milling technology, are critically discussed, highlighting critical aspects used to control their features. Moreover, surface modification and coating techniques are critically examined as tools to enhance biocompatibility, colloidal stability, and targeted delivery. Then, key results in the diverse biomedical applications, namely for oral, skin and pulmonary drug delivery, were discussed. In oral delivery, their capacity to improve drug loading and enable sustained release is emphasized. In skin delivery, aerogels show potential to enhance dermal permeation and provide a sustained release. For pulmonary administration, their low density and aerodynamic properties make them ideal for deep lung deposition. By bridging particle engineering with therapeutic functionality, this review highlights the unique features and advantages of aerogel particles to become the next-generation aerogel-based therapeutic systems. Finally, the current challenges to be addressed and future trends are identified.

## 1. Introduction

Aerogels are defined as low-density solid materials with high porosities, open pore structures, and high specific surface areas. Firstly discovered in 1931 by Kistler (Kistler, 1931), the research on this promising material is gaining a significant growing interest. Due to their unique physicochemical features, aerogels are applied across a broad spectrum of fields, from thermal insulation (Feng et al., 2025),

electrochemistry (Rolison et al., 2023) to biomedical (Keil et al., 2024) applications. Depending on the precursor's source, aerogels can be classified as organic – originating from carbon, natural (e.g., cellulose, starch, chitosan and alginate) or synthetic (e.g., polyurethane, urea-formaldehyde and polyimide) polymers–, inorganic (typically silica, calcium phosphates, alumina and titania) or hybrids (Fig. 1). Namely, aerogels obtained from natural polymers are particularly important in the biomedical field due to their biocompatibility and biodegradability.

*Abbreviations:* AI, Artificial intelligence; Alg, Alginate; AP, Air pressure; API, Active pharmaceutical ingredient; BDP, Beclomethasone dipropionate; CLT, Coating layer thickness; Dex, Dextran; Dex-CHO, Dextran aldehyde; DoD, Drop-on-demand; DPI, Dry powder inhalers; ECD, Electrochemical deposition; FDA, Food and Drug Administration; GAS, Gas antisolvent; GDL, Glucono- $\delta$ -lactone; GMP, Good Manufacturing Practices; GRAS, Generally Recognized As Safe; HA, Hyaluronic acid; HCQ, Hydroxychloroquine; HPC, Hydroxypropyl cellulose; HPMC, Hydroxypropyl methylcellulose; MIC, Minimum inhibitory concentration; PCA, Precipitation compressed antisolvent; PEG, Polyethylene glycol; pMDIs, Pressurized metered-dose inhalers; PVA, Polyvinyl alcohol; SCD, Supercritical deposition; SGF, Simulated gastric fluid; SIF, Simulated intestinal fluid; SMIs, Soft mist inhalers; SS, Salbutamol sulphate; W/O, Water-in-oil.

\* Corresponding author at: AerogelsLab, I+D Farma Group (GI-1645), Department of Pharmacology, Pharmacy and Pharmaceutical Technology, Faculty of Pharmacy, iMATUS and Health Research Institute of Santiago de Compostela (IDIS), Universidade de Santiago de Compostela, E-15782 Santiago de Compostela, Spain.

E-mail address: [carlos.garcia@usc.es](mailto:carlos.garcia@usc.es) (C.A. García-González).

<https://doi.org/10.1016/j.ijpharm.2026.126722>

Received 2 December 2025; Received in revised form 29 January 2026; Accepted 24 February 2026

Available online 28 February 2026

0378-5173/© 2026 The Author(s). Published by Elsevier B.V. This is an open access article under the CC BY license (<http://creativecommons.org/licenses/by/4.0/>).

Although natural polymer aerogels are not yet commercially available in medical products, they have shown strong potential in experimental drug delivery systems (García-González et al., 2021), wound dressings (Bernardes et al., 2021), and scaffolds (Lázár et al., 2023). Additionally, biopolymer aerogels are also being explored for food applications (Manzocco et al., 2021). In particular, aerogels in the microparticle form can be engineered as advanced carriers to overcome some limitations in current drug delivery systems for pulmonary, oral or topical administration (García-González et al., 2021). Their high mesoporosity (i.e. pores between 2 – 50 nm) enables a high drug loading and water uptake, as well as excellent aerodynamic properties. These features can reduce dosing frequency, enhance therapeutic efficacy, and protect sensitive compounds from degradation until reaching the target site (Pantić et al., 2021).

Aerogel particle design is usually integrated into the conventional sol-gel processing steps to produce organic, inorganic and hybrid aerogels – namely, solution preparation, gelation (or coagulation), solvent exchange, and drying (Fig. 1) (Dervin and Pillai, 2017; García-González et al., 2021; Payanda Konuk et al., 2023). Briefly, a solution (sol) is prepared by dissolving or dispersing an organic or inorganic precursor in an appropriate solvent. Subsequently, a physical or chemical crosslinker is introduced to generate a 3D-porous wet gel network between the dispersed chains. Then, the liquid inside the gel pores is directly or stepwise replaced with another solvent (usually water is replaced by an alcohol or acetone) to obtain the so-called lyogel (alcogel if the solvent is an alcohol, typically ethanol). At the drying step, the solvent filling the pores of the lyogel is removed and replaced with air without collapsing the porous structure. Different drying methods are available, such as ambient drying (through the springback effect (Zemke et al., 2022)), freeze-drying and, supercritical drying (Carracedo-Pérez et al., 2024).

However, freeze-drying usually produces cryogels with high macroporosity and low specific surface area, attributed to the solvent crystallization and the volumetric expansion of ice during the process (Betz et al., 2012). On the other hand, ambient drying typically leads to xerogels, characterized by collapsed pore structures attributed to the capillary stresses during the solvent evaporation, resulting in low porosity and also reduced surface area. In contrast, supercritical drying (using typically CO<sub>2</sub>) stands out as the preferred technique as it allows the removal of the solvent ensuring the preservation of the inner porous network structure (Rodríguez-Dorado et al., 2019). During this aerogel production workflow, the shape and size of the resulting aerogel particles can be controlled either during gel production or through post-processing (e.g., coatings and milling).

Given the growing need for advanced drug delivery systems to address complex health challenges, this review aims to provide a systematic and updated overview of current aerogel particle fabrication methodologies identifying the most recent progresses in the field (Section 2). It also evaluates the performances of these particles specifically for pharmaceutical and other biomedical uses with a particular attention to oral, transdermal, and pulmonary drug delivery (Section 3). Finally, future trends and critical research needs on particle engineering to support the ongoing developments and clinical translation of aerogel-based therapeutic platforms are outlined (Section 4).

## 2. Engineering and functionalization of aerogel particles

Shape, size, composition, space component distribution, bioactive compound loading capacity, and bioactive-matrix interactions are the main parameters influencing the performance of aerogels in biomedical applications (García-González et al., 2021). In the next subsections,

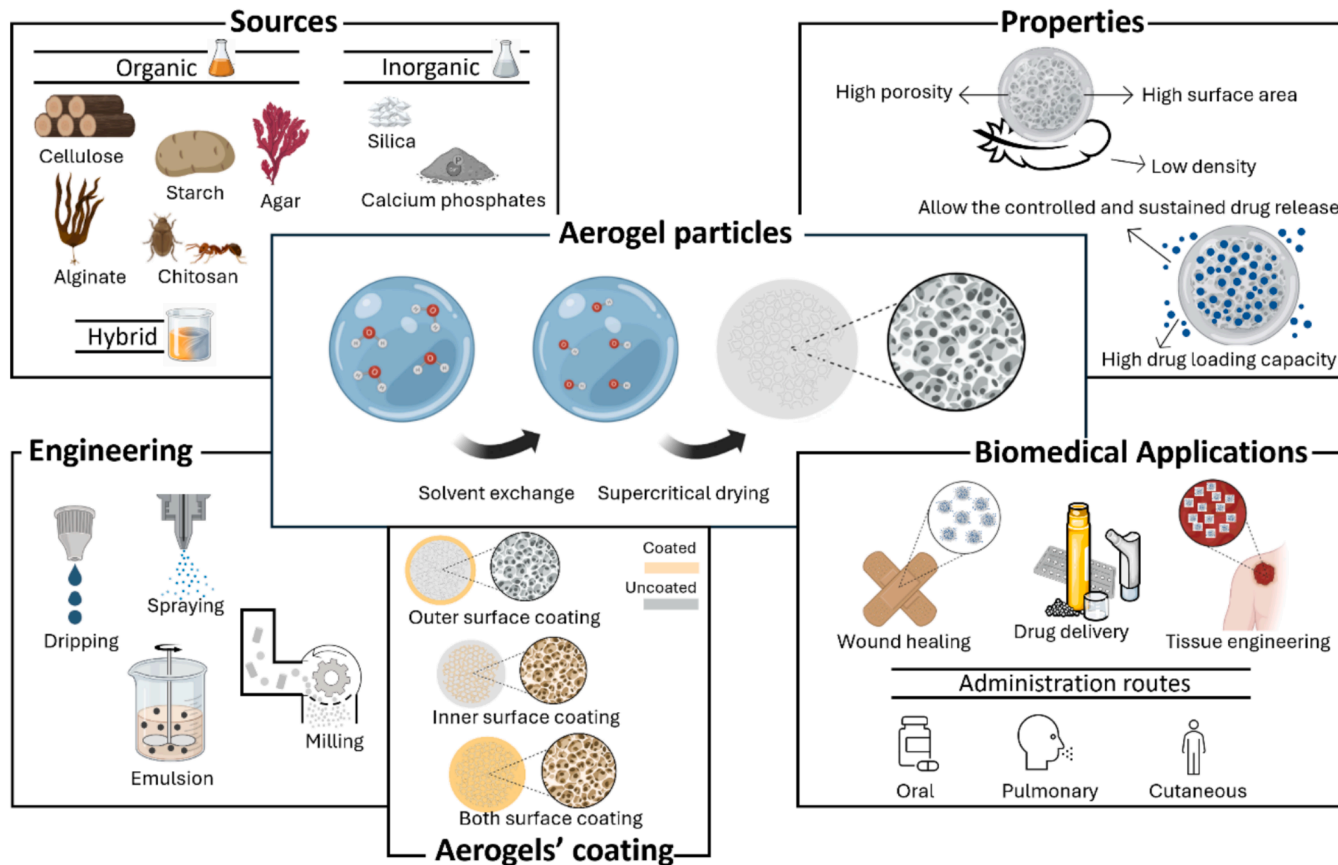


Fig. 1. Overview of aerogel particle engineering workflow: from raw materials to biomedical applications.

current strategies for fabricating aerogel particles will be explained from the technological fundamentals' perspective and supported with selected examples.

The shape and size of the final aerogel formulations can be controlled at different stages of the bioaerogel production workflow. Different bottom-up particle preparation techniques, referring to methods in which wet gel particles are directly formed from polymeric solutions, can be employed prior or during the gelation step (cf. Section 2.1.1) depending on the target size (from micrometres to few millimetres, Fig. 2), often leading to spherical or rounded particles with narrow particle size distributions (García-González et al., 2021; Ganesan et al., 2018). Microparticles can be typically obtained by applying emulsion-gelation (García-González et al., 2012; Ulker and Erkey, 2014), while larger particles can be formed via air-phase droplet methods (via extrusion or dripping), such as spraying (Duong et al., 2024a), dripping (Menshutina et al., 2017) or jet cutting (López-Iglesias et al., 2020). Alternatively, particles can be produced via a post-gelation top-down approach. In this methodology hydro-, alco- or aerogel particles or monoliths are milled (Schroeter et al., 2023) (cf. Section 2.1.2), however, particles with irregular shapes and broad size distributions are typically obtained. Finally, in certain cases, the aerogel particle design may still require further optimization through coatings of the aerogel structures to enhance the controlled drug release behaviour or to provide protection against external environments upon storage or use (García-González et al., 2021; Akgün et al., 2023; Aramideh et al., 2023; Izadi et al., 2023) (cf. Section 2.2).

## 2.1. Technological strategies for aerogel particle production

### 2.1.1. Bottom-up engineering approaches

**2.1.1.1. Emulsion.** Emulsification is a widely employed technique for the preparation of gel particles due to the stable, reproducible and controllable particle size of the obtained emulsions, its relative low process duration and the straightforward potential for scale-up (Zhai et al., 2016). This technique uses a combination of at least two immiscible liquid phases (dispersed and continuous phases) to prepare the emulsion, typically a water-in-oil (W/O) system. The dispersed phase consists on droplets from a gel precursor solution, commonly water-based solution or a suspension containing the gel precursor. The continuous phase is usually an oil. The continuous homogenization of the emulsion by stirring and the use of emulsifiers are common practices to stabilize the droplets of the dispersed phase and prevent their agglomeration (Ganesan et al., 2018). Gelation of the droplets is subsequently induced either by introducing a chemical crosslinker, or by adjusting external physical parameters such as pH or temperature

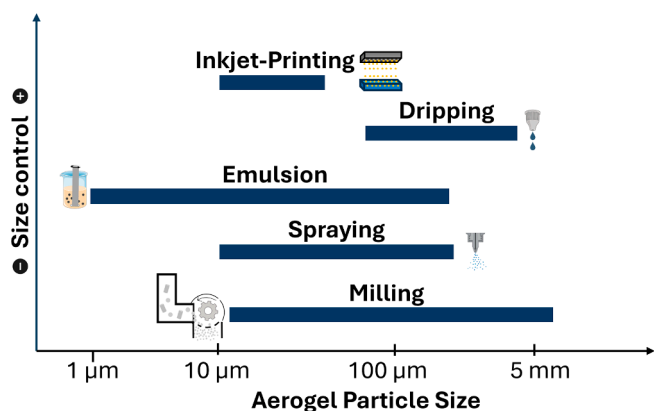


Fig. 2. Comparison of aerogel particle size ranges obtained from the use of each engineering technique and the corresponding control over particle size (lower size control means higher heterogeneity among the size distribution).

(Alnaief et al., 2011). The resulting hydrogel particles are typically submitted to the solvent exchange and supercritical drying steps to obtain the aerogel particles. A schematic representation of the emulsification process is shown in Fig. 3a. The emulsification method enables the production of ultra-fine aerogel particles as small as ca. 2 µm (Duong et al., 2024b). Although emulsification allows precise control over particle size and shape, it requires multiple processing steps and a post-processing gelation, as previously detailed, and even minor variations in the procedure can significantly affect the final particle properties, as it will be discussed below. The main features of the emulsion technique are highlighted in Table 1.

The physicochemical characteristics of the resulting aerogel particles (mainly the size and shape) are strongly influenced by the emulsification parameters, that include the viscosity of both phases, the dispersed-to-continuous volume phase ratio, the stirring speed and mechanism, and the emulsifier type and concentration. Other factors such as polymer concentration in the dispersed phase, the type and duration of cross-linking reaction, and the drying method also play critical roles in the final particle properties (Fig. 3b-d). As an example, alginate (Alg) aerogel microparticles were produced by ionic gelation induced by  $\text{Ca}^{2+}$  ions released from  $\text{CaCO}_3$  within a W/O emulsion (Alnaief et al., 2011). In the same study, the gelation with  $\text{CaCl}_2$  was also tested with significant differences in the properties of the resulting particles. Alg particles crosslinked with  $\text{CaCl}_2$  exhibited agglomeration and irregular shapes (Fig. 3d). In contrast, the use of  $\text{CaCO}_3$  improved the morphology, leading to the formation of more spherical particles (Fig. 3e). This effect was achieved by adding acetic acid to the system to slowly release  $\text{Ca}^{2+}$  ions, promoting a gradual gelation. In general, gel particle sizes were reduced by increasing the stirring speed and surfactant concentration, due to higher energy inputs and the shear-thinning behavior of the polymer solutions (García-González et al., 2021; Alnaief et al., 2011). As an example, Alg particles were produced using two different W/O emulsion gelation mechanisms (M2a and M2b, Fig. 3f-i), which differed primarily in the mechanism used to reduce the pH of the solution – glacial acetic acid was used in M2a, while glucono-δ-lactone (GDL) was used in M2b –. Two different surfactant concentrations (1 vol.% and 5 vol.% Span® 80) were also tested for each mechanism. M2a gelation mechanism resulted in less aggregated spherical particles compared to M2b (Alnaief et al., 2011). Moreover, a higher surfactant concentration (5 vol.% Span® 80) was required in mechanism M2b to obtain uniform spherical particles (Fig. 3h,i). In other example, Alg particles decreased the average size from ca. 51 to 22 µm when the stirring speed increased from 850 to 1200 rpm (Athamneh et al., 2019). An increase in the surfactant concentration also led to a reduction in the average size for starch aerogels (García-González et al., 2012). However, the textural properties, such as specific surface area and porosity, depended more on the sol-gel processing parameters than on the emulsion production conditions (Athamneh et al., 2019; Athamneh et al., 2021; Poncelet et al., 1992).

The selection of hybrid and multi-component systems can also improve the formulation of aerogel particles via the emulsification method, particularly in terms of powder flow properties and biological performance. As an example, the addition of hyaluronic acid (HA) in Alg-HA aerogel microspheres increased the surface charge of the particles, thus enhancing the electrostatic repulsion between particles and reducing their agglomeration (Fig. 3j-m) (Athamneh et al., 2021). Moreover, the incorporation of HA also anticipates an enhancement in the biodegradability of the aerogel particles.

**2.1.1.2. Dripping.** Dripping is a technique used to produce gel particles with high sphericity that essentially consists of extruding a solution through a nozzle at a certain flow rate into a crosslinking solution (Lee et al., 2013). There are different modalities depending on the physical mechanism used to promote the drop formation. In the conventional dripping (Fig. 4a), solutions are extruded through simple nozzles or

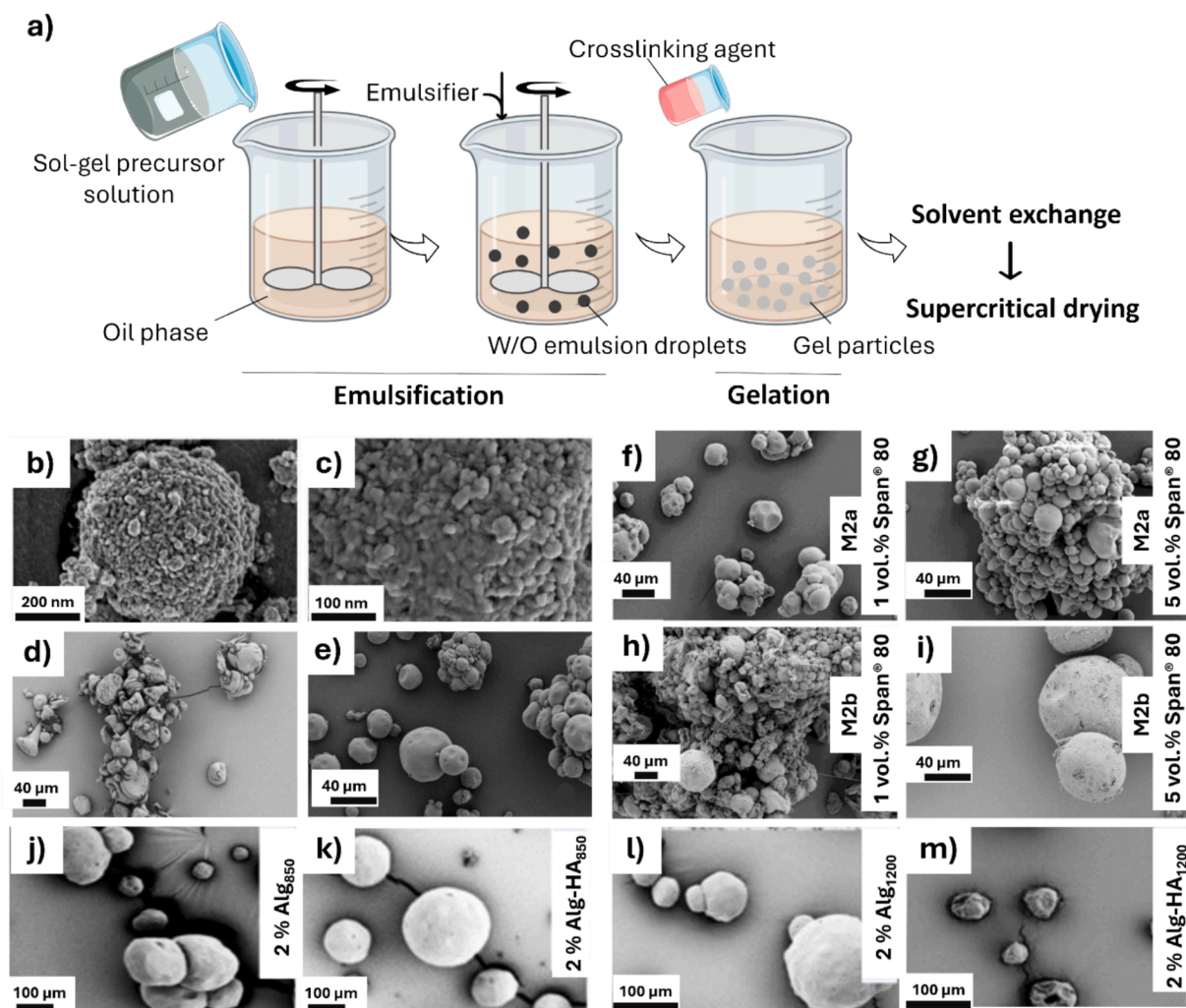


**Fig. 3.** Production of aerogel particles by the emulsification process. (a) Schematic representation of the process. (b,c) Morphological appearance of Alg aerogel particles obtained by gelation-emulsification, adapted from (Duong et al., 2024b) with permission. (d,e) Effect of crosslinker type on particle morphology: (d)  $\text{CaCl}_2$  leads to agglomerated, irregularly shaped alginate aerogels, while (e)  $\text{CaCO}_3$  reduces aggregation, adapted from (Alnaief et al., 2011) with permission. (f-i) Influence of surfactant concentration (1 and 2 vol.% Span® 80) and emulsification parameters (M2a and M2b) on Alg particle size distribution, adapted from (Alnaief et al., 2011) with permission. (j-m) Effect of gel precursor composition (e.g., Alg vs Alg-HA) on final particle properties, adapted from (Athamneh et al., 2019) with permission.

syringes, until gravity forces prevail to the capillary forces between the tip of the nozzle and the solution, promoting the dripping. The main processing parameters of this technique are polymer viscosity, distance between nozzle and crosslinking bath, nozzle characteristics and gravitational forces (Ching et al., 2017). Monodisperse particles with sizes above 1–2 mm can be obtained at low production rates by the optimization of these process parameters (Fig. 4a) (Tkalec et al., 2016). The simplicity of the conventional dripping makes it a versatile technique to optimize crosslinking strategies or gel production for a wide range of biomedical applications (Wang et al., 2025).

Different strategies were implemented to overcome the throughput and particle size limitations of this technique. As one example, systems based on multiple nozzles operating in parallel with continuous extrusion were considered (Brandenberger and Widmer, 1998). Alternatively, vibrational and electrostatic dripping methods can increase the drop formation throughput, but they are only compatible with low viscosity solutions (Prüsse et al., 2008). In the vibrational dripping technique (also called prilling) (Fig. 4b), a vibration device is coupled in the nozzle to promote the drop breakup of the extruded solution at a specific vibration frequency (Whelehan and Marison, 2011). The critical parameters of this technique to obtain spherical particles of uniform sizes are

the vibration frequency (providing the energy to break up the extruded solution in particles) and the dynamic viscosity (values must be lower than few hundreds of mPa·s) (Whelehan and Marison, 2011; Auriemma et al., 2020). As an example, alginate particles with monodisperse sizes of ca. 2 mm for ketoprofen drug release were produced by this technology (Fig. 4b) (Cerciello et al., 2015). Electrostatic dripping (Fig. 4c) is based on the application of a voltage between the tip of the nozzle and the crosslinking bath, generating an electrical field that ejects the extruded solution to the crosslinking solution (Doméjean et al., 2017; Poncelet et al., 1994). The power of the electrical field is the main variable that affects the particle size, reaching spherical Alg particles in the range of 170–400  $\mu\text{m}$  when a voltage difference of 5–6 kV is applied (Poncelet et al., 1999). Other variables that contribute to the morphology of particles are the nozzle diameter, falling distance, viscosity and flow rates of the dropped polymer solution. This technique yields more spherical and uniform particles (Morales et al., 2024), however, to the best of our knowledge, limited data are available on aerogel particles produced by this technique.

Jet-cutting dripping (Fig. 4d) uses a wired (or perforated) rotating disk at high speed to break a jet liquid extruded from a nozzle into droplets (Prüße et al., 1998). It can operate at high flow rates including

**Table 1**  
Summary and technical comparison of aerogels particle production techniques.

Production Method	Sphericity	Throughput	Scalability	Main Advantages	Main Drawbacks
Emulsion	●●●	●●○	●●○	Well-established technique; Easy to scale-up	Post-processing gelation; Multi-step process; Additional steps for oil removal are required
Dripping	Conventional	●●● ●○	●●○	In situ gelation; Simplicity and easy to execute; Do not require complex equipment	Limited size downscaling; Low production capacity; Only compatible with low viscosity solutions
				Vibrational	Ease of producing uniformly sized spherical particles; Higher throughput
	Electrostatic	Easy to obtain spherical particles of uniform sizes; Increase the drop formation throughput	Only compatible with low viscosity solutions		
	Jet-Cutting	High production rate; Compatible with highly viscous liquids	Moderate material losses during processing		
	Air-assisted	Higher throughput and potential to scale-up	Only compatible with low-to-medium viscosity solutions		
Spraying	●●○	●●●	●●●	In situ gelation; Continuous process; Easy to scale-up	Particle aggregation tendency
Inkjet-Printing	●●●	●○○	●○○	In situ gelation; Extremely fine control; Low aggregation rate	Limited scalability; Nozzle clogging; Low productivity
Milling	●○○	●●●	●●●	Easy to scale up	Payload integrity may be compromised; Broad particle size distribution; Loss of structural properties

solutions with medium-to-high viscosity to produce gel particles typically in the 0.5–2.0 mm range (Prüsse et al., 2008). The disk rotating speed, the extrusion rate, the wire distance, nozzle diameter and polymer solution properties strongly influences the mean size, size distribution and shape of particles. As an example, chitosan aerogel particles with spherical shape and sizes around 750–900 μm were prepared with 40-wired cutting disks under rotatory speeds of 6,000 rpm (Fig. 4d) (López-Iglesias et al., 2020). Spherical particles under 500 μm were also reported when polymer concentration, rotatory speed and nozzle diameter were properly selected (Schroeter et al., 2021a).

Finally, air-assisted dripping (Fig. 4e) enables the formation of particles with controlled size, typically ranging from 0.5 to 2.0 mm, by using compressed air to assist droplet generation (Carrêlo et al., 2023; Workamp et al., 2016). The most relevant variables to obtain particles within specific size ranges and homogeneous size distributions are the airflow and the pump flow of the dropped solution, however, excessive airflow may shift the process from a dripping regime to a spray-like regime, representing a key operational limitation of this technique. The composition of the polymer solution can also influence the shape and size distribution of the particles (Carrêlo et al., 2023). This dripping method cannot be operated with highly viscous solutions or at high flow rates (Prüsse et al., 2008).

Despite its versatility and precise control over particle shape and size, dripping techniques typically have low-to-mid throughputs and may be limited to low or moderate viscosity solutions (Table 1). Some of these strategies also require careful optimization of multiple process parameters to achieve monodisperse and spherical particles. Currently, prilling and air assisted dripping are the preferred techniques to scale-up the process.

Nozzle configuration influences the particle design and size of the obtained gel particles for any of the aforementioned dripping technique. Beyond the standard single-nozzle setups used in dripping, more complex designs such as coaxial nozzles allow for advanced particle architectures, such as core-shell particles (Fig. 4f,g). A coaxial nozzle consists of two concentrically aligned channels of different diameters, where the inner nozzle is inserted within the outer one. When two different solutions are independently extruded through each nozzle region into a crosslinking bath, core-shell particles can be obtained. This configuration enables a straightforward, one-step production of encapsulated structures, allowing control over parameters such as particle size and

shell thickness. This configuration can be operated by air-assisted (Fig. 4f) (Ozemes Taylan et al., 2025) or vibrational (Fig. 4g) (Auriemma et al., 2020) technologies. The precise tuning of several operating variables for each solution stream (e.g., solution concentrations, nozzle diameters, and flow rates) is essential to achieve particles with the desired properties and may need advanced multivariable optimization tools (Illanes-Bordomás et al., 2025; Rodríguez-Dorado et al., 2018). Additionally, the crosslinking bath must be compatible with both sol-gel formulations. This versatile and scalable approach facilitates the development of functionalized core-shell aerogel particles with potential for controlled drug delivery (Illanes-Bordomás et al., 2025; Illanes-Bordomás et al., 2023).

**2.1.1.3. Spraying and spray gelation.** Spraying is an atomization process where a bulk liquid is firstly transformed in a dispersion of small particles in a gaseous phase (O'Sullivan et al., 2019; Wanning et al., 2015; Zafar et al., 2024). In spray gelation technique, wet gel atomized particles are produced by the spraying of the droplets in a crosslinking bath (Fig. 5a). These techniques can be used for the production of particles or coatings (section 2.2) of pharmaceutical formulations.

The atomization process uses atomizers, which are devices that promote the droplet formation from a bulk liquid, by different atomization mechanisms (Lefebvre and McDonell, 2017). In the air-assisted atomizers, there are coaxial nozzles where the polymer solution is extruded through the inner channel and compressed air is expelled through the outer channel to break up the liquids into small droplets. In pressure atomizers, the liquid is pumped at high pressures able to break up the capillary forces of the liquids at the nozzle (Omer and Ashgriz, 2011). Rotatory atomizers have a nozzle with a rotatory disk in the tip, promoting the droplet formation by the action of centrifugal forces (Bordón et al., 2021; O'Sullivan et al., 2019; Lefebvre and McDonell, 2017). The selection of the atomizer depends on the sprayed material (viscosity, presence of solids, composition), the target droplet size and size distribution, as well as the target production parameters like the desired flow rate or the energy consumption during the operation (Omer and Ashgriz, 2011). To the best of our knowledge, only air-assisted atomizers were tested to obtain aerogels for biomedical uses (Duong et al., 2024a). This process can be operated/performed in a single spraying production unit that integrates all the required components. More specifically, two lines, one incorporating the container where the polymer

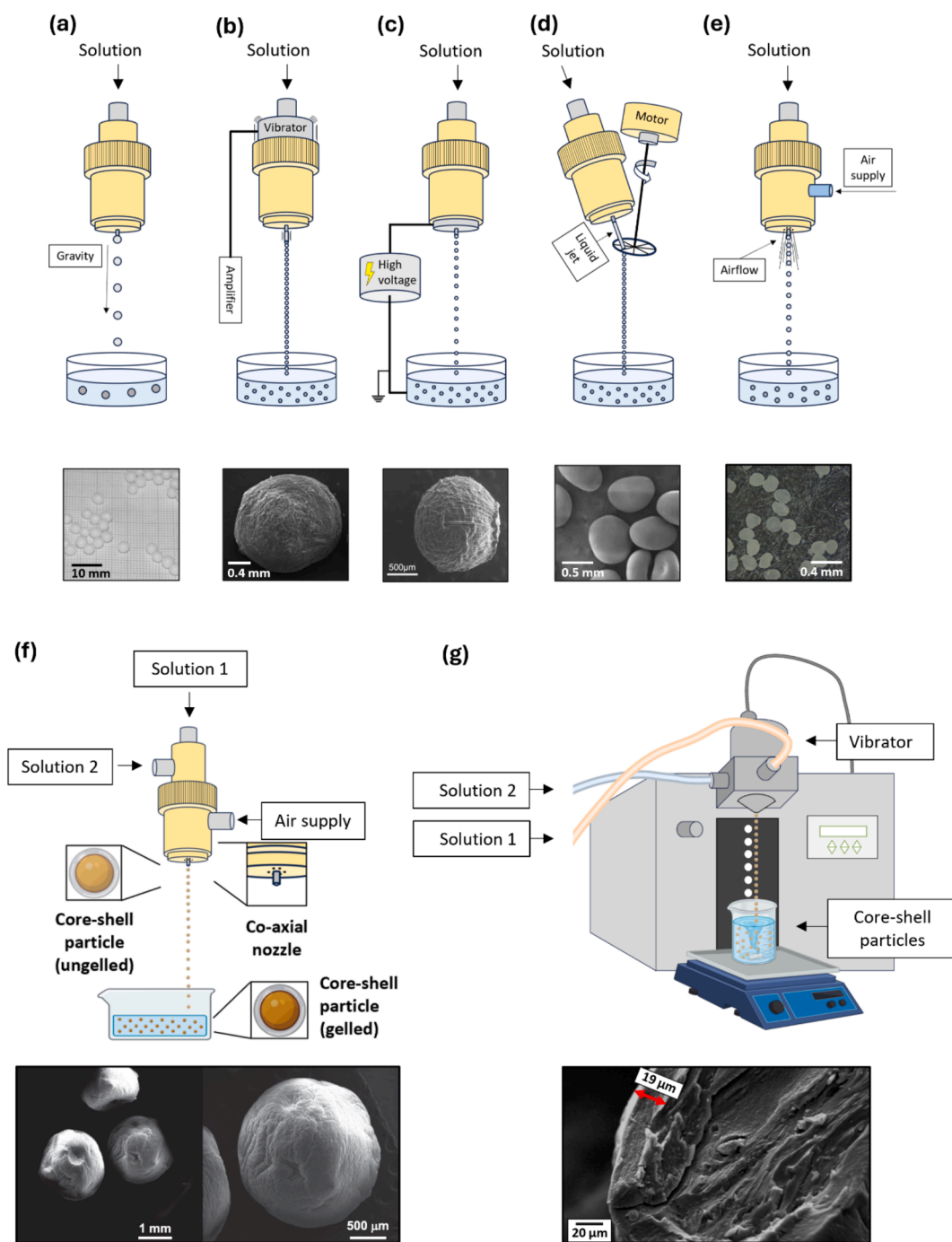


**Fig. 4.** Different dripping strategies to prepare gel particles supplemented with selected examples: (a) Conventional dripping and resulting pectin hydrogels prepared by this technique, adapted from (Tkalec et al., 2016) with permission; (b) vibrational dripping and resulting Alg aerogels, adapted from (Cerciello et al., 2015) with permission; (c) electrostatic dripping and resulting pectin hydrogel beads, adapted from (Morales et al., 2024) with permission; (d) jet-cutting dripping and resulting chitosan aerogels, adapted from (López-Iglesias et al., 2020) with permission and (e) air-assisted dripping and Gellan Gum/Alg particles produced by this technique, adapted from (Carrêlo et al., 2023) with permission. Modifications of these techniques include (f) coaxial air-assisted dripping (e.g., for coated aerogels) (extracted from (Ozesme Taylan et al., 2025; Illanes-Bordomás et al., 2025) with permission), and (g) coaxial vibrational dripping (e.g., for core-shell pectin-alginate aerogels, adapted from (Auriemma et al., 2020) with permission).

solution (e.g. chitosan solution), and the other corresponding to the compressed air supply are designed to converge in the atomizer. Using a peristaltic pump the polymer solution achieved the atomizer specifically positioned at the top of another container containing the crosslinking bath. This one is continuously stirred to avoid particles agglomeration. Once all the solution has been sprayed, the resulting gel particles can be

transferred via another connected line to an additional container with also a stirring mechanism to allow complete reticulation. This process has potential to be scaled-up with a high throughput. Chitosan and albumen gel microparticles were produced via this methodology, followed by  $\text{scCO}_2$  drying (Menshutina et al., 2023). The resulting aerogels exhibited a high specific surface area, high porosity, large pore volume

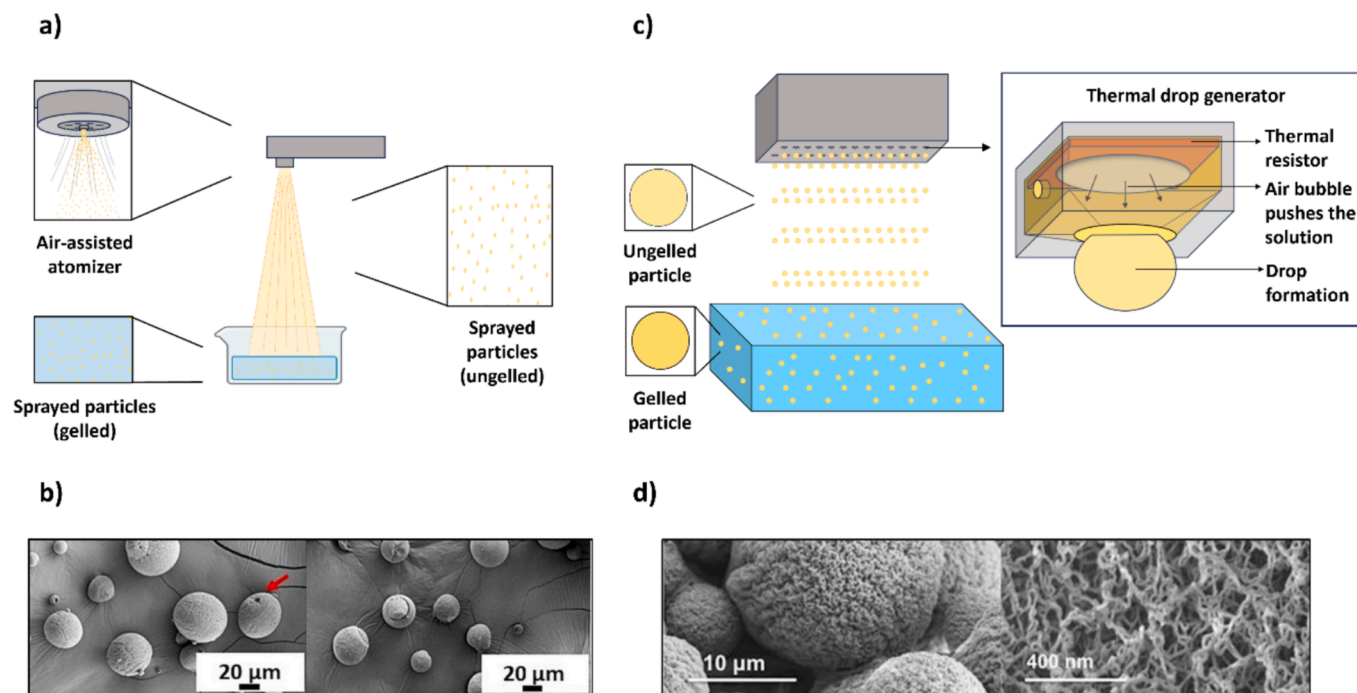


Fig. 5. Aerogel particle production using spraying and inkjet printing: (a) Scheme of spray gelation technique and (b) resulting Alg aerogel particles after  $\text{scCO}_2$  drying (adapted from (Duong et al., 2024a) with permission). (c) Scheme of thermal inkjet printing technique based on drop-of-demand and (d) resulting Alg aerogel particles (adapted from (López-Iglesias et al., 2019a) with permission).

and an aerodynamic diameter compatible for nasal spray drug delivery application.

Some studies have focused on evaluating the influence of the atomization process parameters on the final hydrogel particle size, particularly the influence of solution concentration, feed flow and compressed airflow rates (Cui et al., 2001; Perrechil et al., 2011). These studies generally reported that the mean particle diameter decreased when airflow rates increased. Furthermore, at constant airflow and feed flow rates, a reduction in solution concentration also leads to smaller particle sizes. Alginate aerogel particles in the 37–107  $\mu\text{m}$  range were produced by spray gelation technique from an Alg solution with five different airflow rates (30, 35, 40, 45 and 50  $\text{mL min}^{-1}$ ) and two different pump flow rates (300 and 750 rpm) in a crosslinking bath of  $\text{CaCl}_2$  0.15 M (Duong et al., 2024a). After ageing, the gels were dried with  $\text{scCO}_2$ . It was observed a reduction of aerogel sizes when airflow rate increased and the shape remained almost spherical for all batches. The optimal batch was loaded with a drug (beclomethasone dipropionate, BDP) by supercritical impregnation technique after  $\text{scCO}_2$  drying, resulting in BDP-loaded aerogels with high specific surface areas ( $> 250 \text{ m}^2 \text{ g}^{-1}$ ), interconnected mesoporosity and excellent flowability (Fig. 5b).

Spray gelation enables the production of very small, spherical particles with controlled size (Table 1). However, particle aggregation may occur and must be carefully controlled by adjusting process parameters, such as stirring speed. It is required specialized but not complex atomization equipment that can be easily incorporated in a production unit. The technique can be energy-intensive and a high solution viscosity can be a limitation. However, the right optimization of the particle production makes this technique one of the most promising approaches for scale-up.

**2.1.1.4. Inkjet printing.** Inkjet printing is a material deposition technology where small drops (nanoliter to picoliter range) of a material are expelled from a capillary nozzle into a surface (Scoutaris et al., 2016). This technology has been adapted for the fabrication of aerogel microparticles for biomedical applications. Inkjet printing can be carried out by continuous or drop-on-demand (DoD) methods. Continuous inkjet

printing has fast production rates but low printing quality, reducing their interest in biomedical applications where controlled size and shape are required. DoD inkjet printing can be obtained through two main methods: piezoelectric or thermal drop generators. A piezoelectric drop generator uses a piezoelectric actuator that deforms the cavity of the solution in response to an electrical signal, creating pressure pulses that force tiny droplets of liquid through the fine nozzles of the printhead. Thermal drop generator uses a resistor to heat the solution, expand their volume and produce an individual drop through a nozzle in the printhead (Fig. 5c) (de Gans et al., 2004). These thermal resistors are able to produce individual drops in less than 500  $\mu\text{s}$  by inducing a local increase of the ink temperature to more than 300  $^\circ\text{C}$  in the surroundings of the resistor and for few microseconds, thus avoiding thermal degradation problems of the printed material (Eslamian and Ashgriz, 2011; López-Iglesias et al., 2019a).

Alginate aerogel microparticles for pulmonary drug delivery were successfully prepared using a thermal inkjet printer followed by supercritical drying (López-Iglesias et al., 2019a). Alg solutions (0.25–0.4 wt %) were dropped from cartridges of the printer to a  $\text{CaCl}_2$  0.5 M solution. The Alg concentration range of the ink was restricted as lower concentrations could not gel and higher concentrations could not be extruded due to clogging of the nozzles. The sphericity of the particles highly depended on the printhead-bath distance and on the volume of the crosslinking bath, obtaining agglomerations at low heights and volumes. For optimal formulations (Fig. 5d), aerogel microparticles with narrow size distributions at ca. 20  $\mu\text{m}$  and appropriate aerodynamic diameters were obtained. Inkjet printing allows a precise control over particle size and narrow size distributions, with typical droplet diameters ranging from 10 to 50  $\mu\text{m}$ , making it particularly suitable for biomedical applications (Shi et al., 2021). However, the technique is limited by low throughputs, high sensitivity to solution viscosity, and risk of nozzle clogging (Table 1). A careful optimization of the printing parameters is required to maintain particle sphericity, and the throughput can be improved using multi-nozzle systems.

### 2.1.2. Top-down engineering approaches

All the abovementioned technologies for the engineering of aerogel particles focus on bottom-up approaches to obtain hydrogels already in the form of microparticles, which are subsequently dried to aerogels. Alternatively, milling emerges as a top-down approach to produce fine aerogel particles from larger hydrogels, alcogels or aerogel particles, or from other 3D-geometries (e.g., cylindrical monoliths or slabs) (Keil et al., 2024). Different milling equipment (e.g., ball mill, jet mill, blade mill, colloid mill) employs distinct comminution mechanisms (mainly impact, compression, friction or shearing forces) to mechanically break down materials into fine particles (Fig. 6a-d).

The production of milled aerogel particles for biomedical uses not only depends on the mechanical design and milling parameters, but also on the characteristics of the initial material prior to milling. Key factors, such as polymer concentration, crosslinking degree, Young's modulus, hardness, internal pore architecture and the stage of the sol-gel process (hydro-, alco- or aerogel), significantly influence the milling outcomes (Schroeter et al., 2023). These factors can directly affect not only particle size and shape, but also critical structural features such as porosity, specific surface area and mesopore volume.

In the absence of consensus on the optimal aerogel milling conditions, the following studies illustrate how variations in the initial gel properties and milling parameters impact the final aerogel particle characteristics. Alg and hybrid Alg/silica aerogel microparticles were successfully obtained via wet milling at different stages of the solvent exchange process, using a colloid mill (Schroeter et al., 2023). Gel particles, previously engineered via jet cutting, were suspended in the respective solvent (demineralized water, EtOH/water mixture or EtOH) and milled at speeds in the 10,000–26,000 rpm range and with various mill gaps (i.e. distance between rotor and stator of 300, 600 and 900  $\mu\text{m}$ ). The resulting microparticles were submitted to the remaining solvent exchange steps and then dried via  $\text{scCO}_2$ . No significant changes in the specific surface area of the Alg-silica aerogels were reported after milling. In the case of Alg gels, changes in microstructure after milling were observed depending on the EtOH content at the time of milling. Accordingly, the milling of pristine hydrogels resulted in a significant increase in mesopore volume and a narrower pore size distribution, likely attributed to the compression applied during the process that reduced the macropores and larger mesopores into smaller ones, consequently changing the native pore structure of the gel. The final

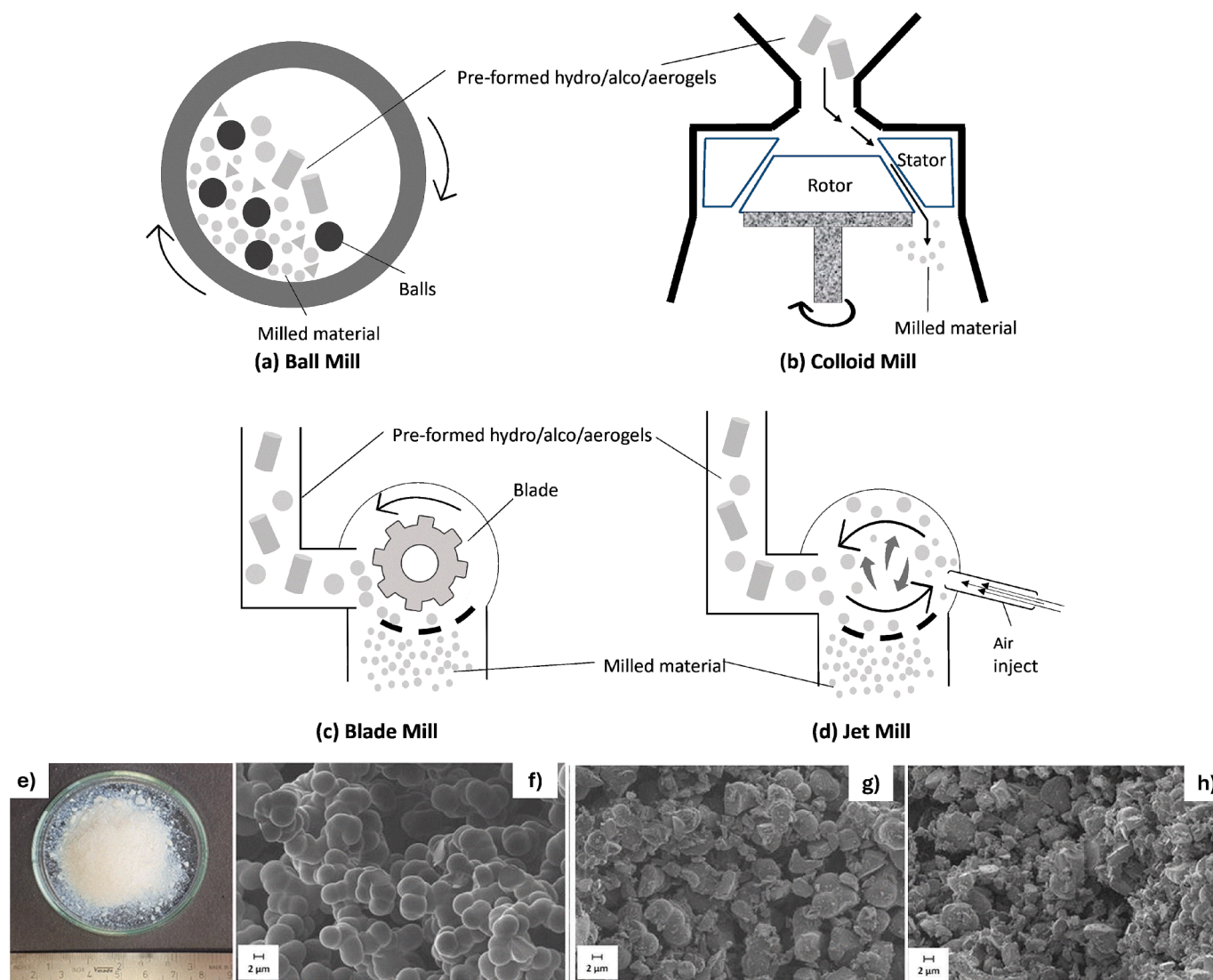


**Fig. 6.** Schematic representation of the four main milling techniques: (a) Ball mill, (b) colloid mill, (c) blade mill and (d) jet mill. (e) Visual appearance of agar aerogel powders ground in a colloid mill, adapted from (Keil et al., 2024) with permissions. (f-h) Carbon aerogel particles obtained by planetary ball milling: SEM images of (f) stiff carbon aerogel monolith consisting of spherical particles of ca. 2–3  $\mu\text{m}$  and macropores; (g) aerogel powder after 5 min of milling (three times) consisting on granules with different sizes and shapes; (h) an increased milling duration (7 min, three times) led to higher homogeneity of granule sizes. Adapted from (Schwan et al., 2020) with permissions.

particle size was influenced not only by technical parameters (e.g., mill gap diameter and speed), but also by the EtOH content of the gel. Specifically, the milling of alcogels results in smaller particles. On the other hand, the sphericity of the resulting particles depended only on the properties of the gel, particularly on the Young's modulus, which was influenced by EtOH content. It was also demonstrated that milling alcogels at higher speeds (26,000 rpm) and with smaller gaps (300  $\mu\text{m}$ ) yielded particles with smaller sizes (ca. 70–100  $\mu\text{m}$ ) and higher sphericity (ca. 0.79). A particle size difference of up to 200  $\mu\text{m}$  was observed between milling Alg hydrogels and alcogels and endorses the milling at the alcogel stage as the most favourable approach.

Comparable patterns were identified in the case of agar aerogel particles obtained by wet milling of cylindrical monoliths of agar alcogels (Keil et al., 2024). These monoliths were firstly crushed using a blender and then ground in a colloid mill (operated at 2,200 rpm with a 900  $\mu\text{m}$  gap). The resulting alcogel particles were subsequently dried with  $\text{scCO}_2$ . Successful drying was achieved only above a certain agar concentration (2–3 wt%) of the respective alcogels (Fig. 6e for 3 wt%). At the microscopic level, the particles exhibited low sphericity and roundness. Although the specific surface area remained high, it was lower than that of the monolithic aerogel source. Regarding mesoporosity, the reported specific mesopore volume (1.0–1.2  $\text{cm}^3 \text{g}^{-1}$ ) was aligned with the typical values for agar aerogels.

In contrast, the milling of dry aerogels has been reported to lead to a loss of porosity and of structural integrity (Schwan et al., 2020). Carbon aerogel microparticles were obtained by milling aerogels (Fig. 6f-h). The milling process successfully reduced the aerogel particle size but also resulted in a densification of the aerogel structure and a decrease in the overall porosity. The mechanical forces involved in the milling of aerogels can disrupt the delicate balance between microporosity and mesoporosity, potentially leading to less effective aerogels for biomedical applications.

Although there is still insufficient consensus on the optimal aerogel processing phase at which milling should be performed, some pharmaceutical aerogel powders obtained by milling dried aerogels have been already investigated as carriers for various bioactive molecules, such as insulin, morphine and sildenafil (Lee and Gould, 2006). Namely, carbon-based aerogels derived from mannitol or trehalose were prepared by a chemical reaction followed by solvent exchange with ethanol. In this case, drug loading was achieved by soaking the alcogel in an alcoholic solution of the desired biomolecule, prior to  $\text{scCO}_2$  drying. The resulting low-density aerogels (0.02–0.05  $\text{g cm}^{-3}$ ) were subsequently milled into fine powders using fluid energy milling in a spiral jet mill. The milling process was coupled with the use of a  $\text{N}_2$  gas flow to maintain low temperatures, thereby preserving the structural and biological integrity of the biomolecules. The final aerogel particles had sizes ranging from 0.5 to 10  $\mu\text{m}$ . However, it is essential to assess the integrity and stability of the bioactive compound, as well as to ensure that no significant mass losses occur during the milling process. Conversely, if the aerogel were in its unprocessed state, i.e. with empty pores, the integrity of the porous structure should be a critical concern, and the milling process should be well tested and planned.

Milling is a simple and widely accessible method for producing aerogel particles, with high throughput and easy scalability, being a promising approach for an industrial scale production (Table 1). However, as a destructive post-processing technique, it generally produces irregular particles with broad size distributions and reduced sphericity. The mechanical stresses involved may partially damage the aerogel network, leading to losses in porosity and surface area. For aerogels loaded with biomolecules or drugs, milling may also compromise payload integrity and release performance. These limitations may hinder its suitability for biomedical applications requiring well-controlled particle morphology and structural integrity.

## 2.2. Coatings of aerogel particles

Relevant research efforts have been dedicated to modifying the surface of aerogels via coating. Indeed, coatings of different nature can be desired in drug-loaded particles to modify the release patterns of the active compound in the administration environment. For example, polymethacrylates polymers (usually denoted by the commercial name Eudragit®) have been tested in a wide range of oral formulations to retain the bioactive compounds in upper sections of the gastrointestinal tract before reaching the ileum or colon sections (Alnaief et al., 2012).

Coating materials can be applied to the outer surface and/or the inner pore surface of aerogels via physical or chemical interactions (García-González et al., 2021). In the outer surface coating approach, the coating material (with coating layer thickness –CLT– typically ranging from a few microns to millimeters) covers the external surface of aerogels without penetrating inside the pores. In the inner pore surface coating approach, a thin film (CLT of typically only few nanometers) is formed on the inner surface of aerogels, including the surfaces of the pores, via preserving the open porous nature of aerogels. Coatings of aerogels can be accomplished either in the outer surface using liquid-based coating methods (spray coating, dip coating and prilling) or both surfaces via solvent-free coating methods (electrodeposition and supercritical deposition) (Salawi, 2022). Table 2 provides a comparative analysis of the advantages and drawbacks associated with these coating techniques when applied to different types of aerogel particles.

### 2.2.1. Spray coating

In the spray coating method, melts, aqueous and organic solvent-based solutions of various polymers and their composites are sprayed on the materials using different equipment, such as fluidized beds, drum coaters and pan coaters (Song et al., 2025). Among them, fluidized beds are mostly preferred since they provide high heat and mass transfer rates, wide range of CLT possibilities (from few microns to few millimetres) and high coating efficiency and reproducibility (Jia et al., 2026).

Studies on spray coatings of aerogels in fluidized beds revealed that there are two main aerogel-specific challenges: (i) their extremely low density often causes unpredictable particle movement during coating and leads to breakage, (ii) direct interaction between aerogels and coating material solutions or melts within the bed can facilitate coating material infiltration into the pores, thereby inducing particle shrinkage.

Fluidized beds are generally classified according to the nozzle position as top spray, bottom spray, and tangential spray. A top spray fluidized bed was first time used to coat Alg/starch aerogels with Eudragit® L 30 D-55 (Antonyuk et al., 2015). Average CLT was  $250 \pm 37 \mu\text{m}$  without visual cracks on the coating layer surface. Even though homogenous coating layers were achieved, shrinkage of aerogels indicated that parts of the pore structure collapsed during the process.

Spouted beds and Wurster fluidized beds, which are two types of bottom spray fluidized beds, have been investigated for outer surface coatings of aerogel particles due to easy handling with particles and flexibility to control the particle velocity (Abdul Halim et al., 2018; Zhou et al., 2019) (Fig. 7). In a spouted bed, fluidization air passes through two adjustable air inlet slits to provide uniform particle fluidization (Fig. 7b) (Alnaief et al., 2012). As opposed, in a Wurster fluidized bed the fluidization air passes through the holes of a perforated plate (Fig. 7d). To prevent random particle fluidization, a cylindrical Wurster tube is placed inside the Wurster fluidized bed, which separates wet and dry particles during the process (Akgün and Erkey, 2019). Wurster tube also divides the fluidized bed in four main zones as illustrated in Fig. 7d.

The first modelling results of coating of aerogels in a spouted bed (Plawsky et al., 2010) demonstrated that equipment geometry was suitable for particle fluidization, but recirculation after a certain processing time may lead to particle agglomeration. This phenomenon was experimentally validated using different polymer solutions (PVA, Eudragit® and polyurethane) to separately coat silica aerogel particles, identifying a maximum boundary condition to prevent aerogel breakage

**Table 2**  
Summary of coating techniques applied to aerogel particles for biomedical applications.

Coating Technique	Coated Surface	Advantages	Drawbacks	Examples		
				Aerogel Type	Coating material	Refs.
Spray Coating	Outer	High reproducibility; Product uniformity; Easy handling with particles; Wide range of coating thickness; Versatility in application	Distortion, cracking and delamination; Shrinkage; Requirements for optimization of hydrodynamic behaviour; Long drying and curing time	Alg	Methacrylic acid-ethyl acrylate; Copovidone/HPC	(Akgün et al., 2023; Akgün et al., 2022)
				Alg-starch	Eudragit® L 30 D-55	(Antonyuk et al., 2015)
				Cellulose	Shellac	(Schroeter et al., 2021c)
				Silica	Eudragit® L/ PEG; Polyurethane, Surelease®, Eudragit®L; Polyvinyl alcohol (PVA)	(Alnaief et al., 2012; Abdul Halim et al., 2018; Plawsky et al., 2010)
Dip Coating	Outer	Homogeneity; Cost-effective; Simple setup; Scalability for batch processing	Shrinkage; Long drying and curing time; Adhesion issues of coating material; Requirements for optimization of coating viscosity and withdrawal speed	Whey protein	Shellac	(Goslinska et al., 2019)
				Alg	Alg	(Veronovski et al., 2013)
				Alg-silica	Alg/HPMC; Silica/HPMC; Silica	(Bugnone et al., 2018)
				Pectin	Chitosan	(Pantić et al., 2020)
				Silica	PEG; Alginate; PVA; Starch & Gelatin	(Aramideh et al., 2023; Afrashi et al., 2019; Giray et al., 2012; Ulker and Erkey, 2014)
Supercritical Deposition	Outer & Inner	Well preserved porous structure; Deep penetration; Uniformity; Environmentally friendly	Limited precursor solubility; High cost; Complex process control; Scaling challenges; Potential for undesired reactions	Starch	Trehalose	(Izadi et al., 2023)
				Silica	Eudragit® RL	(Murillo-Cremaes et al., 2014)

of atomizing air pressure (AP) of 0.8 bar and a coating solution flow rate of  $6 \text{ mL min}^{-1}$ . CLTs were between few microns and 10 nm. A spouted bed was used for the coating of cellulose (Fig. 7a) and whey protein aerogel particles (Fig. 6c) with an ethanolic shellac solution (Goslinska et al., 2019; Schroeter et al., 2021c). In the case of whey protein, aerogel particles between 5 and  $90 \mu\text{m}$  were coated with CLT of up to 700 nm (Goslinska et al., 2019). A gradual increase of the fluidization airflow rate (from 4 to  $10 \text{ m}^3 \text{ h}^{-1}$ ) was needed as the aerogels started to gain mass. In that case, no particle breakage occurred, but the coated aerogels had rough surfaces and showed agglomeration. In another study, cellulose aerogels of sizes between 1.1 and 4.4 mm were coated with shellac with CLT from 10 to  $50 \mu\text{m}$  (Schroeter et al., 2021c). The cellulose content in the aerogel precursor (2 and 6 wt%) influenced the quality of the coating. 6 wt% cellulose aerogels had smooth initial surfaces forming complete coating layers, whereas 2 wt% aerogels, resulted in incomplete coatings with exposed porous structures due to initial defects and high roughness. Particle breakage, agglomeration, and liquid penetration were avoided by carefully controlling the ratio of sprayed solution to the number of particles. A strategy consisting of applying a protective pre-layer before the main coating was able to prevent liquid penetration inside the pores of aerogels during coating (Alnaief et al., 2012). This technique was successfully demonstrated with ibuprofen-loaded silica aerogel particles of  $200 \mu\text{m}$  to few millimeters size. In this process, a molten polyethylene glycol (PEG) solution was sprayed onto the aerogels creating a protective layer with a CLT of  $35 \pm 3.2 \mu\text{m}$ . This initial PEG layer effectively preserved the aerogels' 3D porous structure before the application of the Eudragit® L second layer.

Aerogel coatings in Wurster fluidized beds have traditionally relied on a circulatory particle motion regime which ensures precise particle velocity and prevents unpredictable fluidization, thereby avoiding damage like breakage or agglomeration and preserving 3D porous structure of aerogels during coating (Akgün et al., 2023; Akgün et al., 2022). However, experimental and computational studies on the hydrodynamic behaviour of aerogels in Wurster fluidized beds have identified six different fluidization regimes (Akgün and Erkey, 2019;

Akgün and Erkey, 2021; Antonyuk et al., 2012). Minimum fluidization and bubbling regimes were observed in both tube and annular zones, whereas pneumatic regime existed only in the tube zone. A horizontal circular motion was identified for aerogels in the tube zone. Turbulent and circulatory particle motion regimes were observed in the whole bed. A Wurster fluidized bed was firstly utilized for aerogels to coat silica aerogel particles with an aqueous PVA solution (Abdul Halim et al., 2018). Particle agglomeration was avoided and CLT was of  $50 \mu\text{m}$  after 60 min of processing. However, coating solution penetration inside the pores of aerogels was observed, which caused a slight particle shrinkage. To prevent this, the porous structure of aerogel particles was successfully protected during coating in a Wurster fluidized bed via proper combinations of bed temperature and atomizing AP (Akgün et al., 2022). Alginate aerogel particles were coated with copovidone and hydroxypropyl cellulose (HPC) at a fixed atomizing AP (1.7 bar) and processing time (30 min) (Fig. 7e-h), leading to different coating results depending on the operating temperature. A protected porous structure with a very uniform and high CLT (ca.  $150 \mu\text{m}$ ) was obtained at  $50 \text{ }^\circ\text{C}$  (Fig. 7g), whereas a rough coating layer surface of low CLT (ca.  $50 \mu\text{m}$ ) was achieved at  $30 \text{ }^\circ\text{C}$  (Fig. 7h). These variations were attributed to the rheological changes of the coating polymer solution with temperature, where moderate coating polymer viscosities ( $0.059 \text{ Pa}\cdot\text{s}$ ) led to a good coating solution droplet spreading that resulted in low contact angles and a smooth coating layer surface (Fig. 7g).

Drug-loaded aerogels likely require modified coating procedures in a Wurster fluidized bed compared to the unloaded ones. Their increased fragility upon drug loading makes them less able to tolerate high AP (Akgün et al., 2023). To prevent the fragmentation, it was suggested a coating process strategy for ibuprofen-loaded alginate aerogels consisting on low and variable atomizing AP: initially 1.5 bar for the first 20 min to promote initial weight gain, then reduced to 1.4 bar to minimize particle collisions, and further decreased to 1.3 bar after 30 min and for the remaining coating time (120 min). However, this strategy resulted in a non-linear and slower CLT gain (from  $15.9 \pm 5.5 \mu\text{m}$  to  $84.1 \pm 13.2 \mu\text{m}$  during 180 min) in comparison to the linear CLT increase (from  $25.6 \pm$

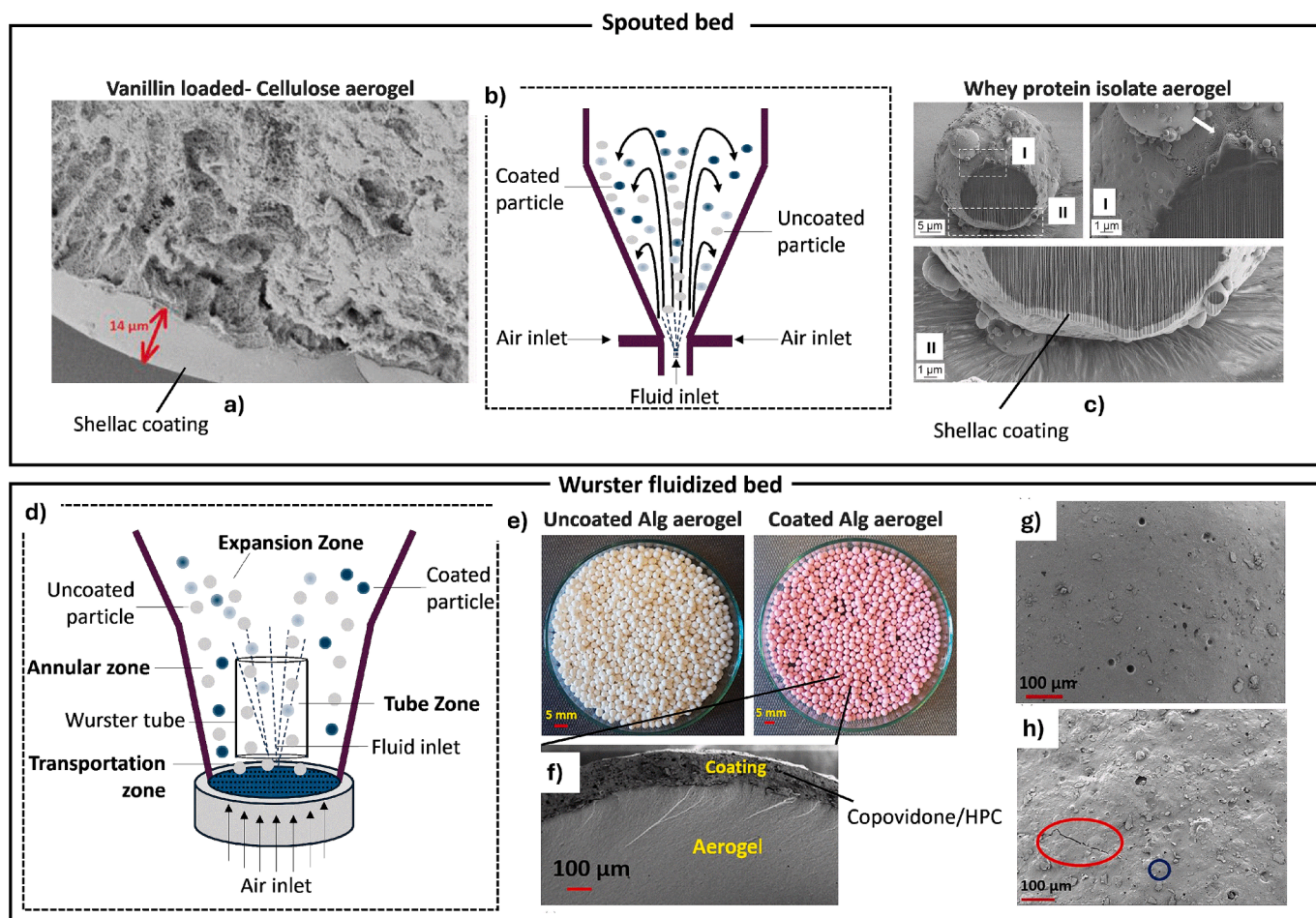


**Fig. 7.** Strategies for the spray coating of aerogel particles: (a-c) Scheme and examples of aerogel particle coating process in a spouted bed and (d-h) in a Wurster fluidized bed. (a,c) Shellac layer and inner part of cut-open aerogel particles coated in a spouted bed, adapted from (Schroeter et al., 2021c) and (Goslinska et al., 2019) with permission. (e) Alg aerogel particles before and after coating with copovidone/HPC polymer mixture (pink) in a Wurster fluidized bed and respective cross-sections showing (f) the inner part, and (g,h) the coating layer morphology adapted from (Akgün et al., 2022) with permission.

7.3  $\mu\text{m}$  to  $53.4 \pm 8.5 \mu\text{m}$  within 50 min) of unloaded alginate aerogel particles at a constant and high atomizing AP (1.7 bar).

### 2.2.2. Dip coating

Dip coating is another method to achieve outer surface coatings where the material to be coated is immersed into a coating solution and then withdrawn to allow to dry. Viscosity of the coating solution,

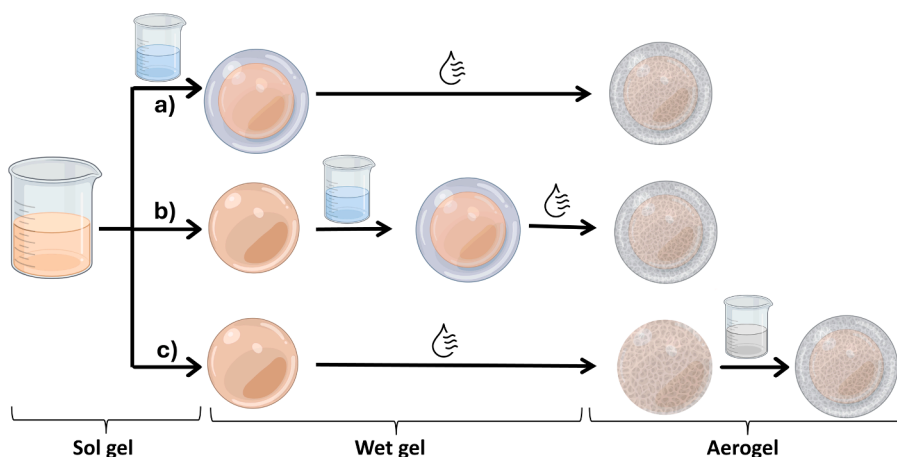


**Fig. 8.** Coating strategies to obtain coated aerogels via dip coating method: (a) Coating during gelation process, before drying, allowing for simultaneous formation of aerogel itself and coating layer; (b) coating after the extrusion step but still before the drying process, where the wet gel is coated, and then both gel and coating material undergo drying together; (c) coating process after drying, for situations requiring less disruption to the fragile aerogel structure, which often utilizes methods specifically designed for porous materials to ensure uniform coverage without pore collapse.

withdrawal speed and immersion time may significantly change CLT and coating layer surface morphology. Dip coating method includes sol-gel coatings, self-assembled monolayers and layer-by-layer coatings (Rajasekar et al., 2025).

Dip coating is used for aerogel production under different strategies for coating gels in both wet and dry states (Fig. 8). Each strategy presents unique advantages in terms of material integrity, simplicity of setup, process control, and the resulting properties of the coated aerogel. Dip coating offers numerous benefits for aerogel particle coating, such as process versatility, homogeneous surface coverage, straightforward setup, batch scalability, and cost-effectiveness (Table 2). Nevertheless, the method faces challenges like extended drying and curing durations (Tyagi and Barman, 2026). Other common issues include aerogel shrinkage, and difficulty in ensuring adequate adhesion of the coating material.

Dip coating method can be used for the coating of aerogels with another aerogel or hydrogel layer (Veronovski et al., 2013; Ulker and Erkey, 2014). The coating of multilayers of Alg on alginate aerogel particles were obtained by dip coating with preserved aerogels' porous structure, avoiding breakage and shrinkage (Veronovski et al., 2013). The synthesized spherical alginate hydrogels were immersed in 0.75 wt % alginate solution and rapidly dipped into 0.2 M CaCl<sub>2</sub> solution to obtain a first alginate layer around the initial hydrogel particles. Hydrogels with 3, 5, and 8 coating layers were obtained via a repeated dipping process. Subsequently, solvent exchange was performed with ethanol, and the coated aerogels were obtained via supercritical drying. A higher Alg solution concentration yielded more compact and stable gels. This procedure allowed the incorporation of a water-soluble drug (nicotinic acid) either within the initial hydrogel particles or within distinct layers, representing a promising approach for spatiotemporal delivery of different drugs.

Aerogels were coated with various polymers via dip coating method, such as PVA (Afrashi et al., 2019), chitosan and gelatin (Aramideh et al., 2023). 10 wt% of aqueous PVA solution at 80 °C was used as a coating solution where drug (fluconazole)-loaded silica aerogels were immersed in this solution, and then dried at 25 °C (Afrashi et al., 2019). After coating, BET specific surface area was 800 m<sup>2</sup> g<sup>-1</sup>, which showed the preservation of the porous structure of aerogels during the coating process. Following a similar strategy, a double polymer coating was applied to silica aerogels via dip coating, using a first chitosan layer and a second gelatin layer (Aramideh et al., 2023). The double coating led to blockage of the pores as the specific surface area was reduced from 436 m<sup>2</sup> g<sup>-1</sup> to 331 m<sup>2</sup> g<sup>-1</sup> after chitosan coating and further reduced to 13 m<sup>2</sup> g<sup>-1</sup> after the second gelatin coating.

Emulsification/internal setting technique was adapted as a new dip coating technique. It was firstly tested to coat hybrid silica-Alg aerogel particles with three different coating layers: Alg/hydroxypropyl methylcellulose (HPMC), silica/HPMC or hydrophobic silica (Bugnone et al., 2018). The coating of hybrid silica-Alg hydrogel or alcogel beads was tested with three different solutions to evaluate coating performance and the potential impact on drug (ketoprofen) loading and release. Uncoated hydro- or alcogel beads impregnated with ketoprofen, were suspended in the coating solution (water phase) and then dispersed in an oil phase under continuous stirring. In the case of Alg/HPMC and silica/HPMC coatings, gelation was achieved by thermal gelation of HPMC. Each coated hydrogel and alcogel particles were subjected to stepwise solvent exchange followed by scCO<sub>2</sub> drying. No characterization of the coating layer or the coated particles was reported in this study, however, it showed good results regarding the drug loading capacity and the release behaviour of the coated aerogel particles. A similar approach was also used for polydimethylsiloxane (PDMS) coating of silica aerogels with a particle size of few microns (Cai et al., 2023). Similarly to conventional dip coating, the emulsification technique has potential to be adapted to obtain multiple coating layers on aerogel particles (Xiang et al., 2025).

### 2.2.3. Supercritical deposition (SCD)

SCD is an effective and eco-friendly method for coating aerogel particles, as it produces no liquid waste and valorises CO<sub>2</sub> (Yousefzadeh et al., 2022). Its mass transfer rates are significantly higher compared to other coating techniques, so that the porous structure of aerogels is well preserved during the process, leading to highly uniform and surface-conforming coatings on the inner surface (Erkey, 2009). A primary limitation of using scCO<sub>2</sub> for coating is the restricted number of coating materials and co-solvents that are sufficiently soluble in scCO<sub>2</sub>. A successful coating layer requires a precise control over pressure, temperature, flow rate, and precursor concentration within the supercritical fluid, which can be complex to manage. The scale-up of SCD processes to industrial production can be challenging due to the inherent difficulties in handling large volumes under high pressure and maintaining uniform conditions.

Coating aerogel particles using SCD is exceptionally rare in the literature, with only one study successfully reporting the coating of drug-impregnated silica aerogels with a Eudragit® RL 100 layer in supercritical CO<sub>2</sub> for biomedical purposes (Murillo-Cremaes et al., 2014). This was accomplished via two distinct antisolvent approaches, the gas antisolvent (GAS) and the semicontinuous precipitation compressed antisolvent (PCA). In both approaches, the coating material (Eudragit® RL 100 layer) is dissolved in an organic solvent (acetone) that upon contact with scCO<sub>2</sub>, that act as an antisolvent, reduces solvent power, causing precipitation of the coating material onto the aerogel. GAS approach involved introducing CO<sub>2</sub> into a high-pressure vessel (100 bar, 26 °C for 1 h) containing silica aerogel particles of 300 nm size and Eudragit® RL 100 in acetone. PCA method entailed dispersing silica aerogels of 65 nm size in the same coating solution and spraying them into a continuous stream of CO<sub>2</sub> (30 °C, 90 bar) within a high-pressure vessel. In both approaches, the coating material completely covered both outer and inner surfaces of the particles. Notably, in both approaches the resulting particles were embedded in a polymer mass, requiring an extra rinsing step with a proper solvent (methanol) to achieve almost individually coated particles. Although, no further optimization of the coating process was explored, it was observed a significantly improved drug release profiles after coating.

## 3. Biomedical uses of aerogel particles

The effectiveness of drug formulations based on aerogel particles is governed by the controlled release and targeted absorption of active pharmaceutical ingredients (APIs) at specific anatomical sites. These biopharmaceutical processes are primarily influenced by critical formulation parameters, including particle size distribution, surface morphology, and the underlying physical phenomena such as matrix erosion, particle disgregation, and gel swelling. Following the comprehensive review of aerogel formulation strategies and surface engineering techniques in Section 2, this section will be devoted to showcase the enhanced drug delivery performance across oral, dermal, and pulmonary administration routes of aerogel particles obtained by these manufacturing approaches.

### 3.1. Oral drug delivery

Oral administration route is commonly used for therapeutic treatments of a wide range of pathologies due to its convenience, patient compliance, and cost-effectiveness (Illanes-Bordomás et al., 2023; Alqhtani et al., 2021). Many drug formulations still face significant challenges when administered orally, including low bioavailability, targeting limitations and instability to the gastrointestinal environment.

Aerogel particles are able to provide enhanced drug solubility and dissolution rates, high drug loading capacities, controlled and sustained release, protection of sensitive drugs and site-specific delivery (García-González et al., 2011). Aerogels can offer a faster drug release (in the order of minutes) than crystalline drugs, which can lead to enhanced

bioavailability (Kumar Rajanna et al., 2015; Obaidat et al., 2018; Smirnova et al., 2005). These enhanced drug release rates with aerogels are due to (i) the high contact surface area between the adsorbed drug inside the pores of aerogels with the body fluid, (ii) the rapid collapse of the aerogel backbone upon contact with the release medium for certain aerogel formulations, and (iii) the drug amorphization or the reduced drug crystal size that can take place when the drug is loaded in an aerogel.

A sustained drug release can also be achieved with aerogels (Smirnova et al., 2005; García-González and Smirnova, 2013). Starch aerogel particles prepared by the emulsion-gelation method were used as carriers for ketoprofen (García-González and Smirnova, 2013). Pure ketoprofen in the crystalline form dissolved 80 % of the drug in PBS pH 6.8 medium within 1 h. In contrast, ketoprofen release from the aerogel particles had an initial fast dissolution of 56 % of the drug in the first 2 h, followed by a sustained release of the remaining drug.

Aerogel-based pH-sensitive drug delivery systems in oral formulations offer a strategic advantage by enabling site-specific delivery within the gastrointestinal tract and protecting pH-sensitive drugs. Polysaccharide aerogel microspheres loaded by impregnation with ketoprofen were obtained from alginate (Fig. 9a) and pectin (Fig. 9b) showing a controlled drug release of the drug in simulated gastric fluid (SGF) (0.1 N HCl, pH 1.2) and in simulated intestinal fluid (SIF) (PBS pH 6.8), in contrast to the dissolution profiles of pure ketoprofen (García-González et al., 2015). Also, *in vitro* release experiments demonstrated that Alg beads had faster drug releases at pH 1.2 than pectin beads, opening the possibility to use different aerogel formulations according to the desired target tissue.

Coated aerogels can regulate the drug release pattern in the gastrointestinal tract at different pHs. In SGF (0.1 N HCl acidic medium), the ketoprofen release from PEG-coated silica aerogels via dip coating was investigated (Giray et al., 2012). An increase in PEG concentration led to a decrease in drug release rate and provided a prolonged release for several days. The effective diffusion coefficients of ketoprofen from aerogels coated separately with 15 and 30 % w/v PEG layers were 0.9 and 0.07 %, respectively. At pH 1.2, three different coating materials (Alg-HPMC, silica-HPMC, and hydrophobic silica) were applied to hybrid silica/Alg aerogel particles by the emulsification/internal setting technique (Bugnone et al., 2018). Coated aerogels, particularly the ones coated with silica, delayed ketoprofen release with 64 % of the loaded drug released in 60 min, whereas 90 % of the drug payload was released after 3 min for the uncoated aerogels. In another example, triflusal-loaded silica aerogels were coated with Eudragit® RL 100 via SCD method (Murillo-Cremaes et al., 2014). In an aqueous 0.01 M HCl medium, triflusal released almost 100 % of the drug in the first 5 min from the uncoated aerogel particles, while the coating of the aerogels prolonged the drug release time to several hours. Similarly, under SIF (PBS pH 5.8) the release profile of paracetamol from conventional silica aerogels and Alg aerogel-coated silica aerogels was investigated (Ulker and Erkey, 2014). The Alg aerogel layer (CLT of 4 mm) prevented the immediate collapse of the porous structure of silica aerogels when contacted with the PBS medium leading to a decrease in the release rate (90 and 75 % of paracetamol released from conventional aerogels and the coated aerogels in 50 min, respectively). In another study, the chitosan coating of pectin aerogels prolonged the complete curcumin release up to 24 h at pH 6.8, while complete curcumin release from

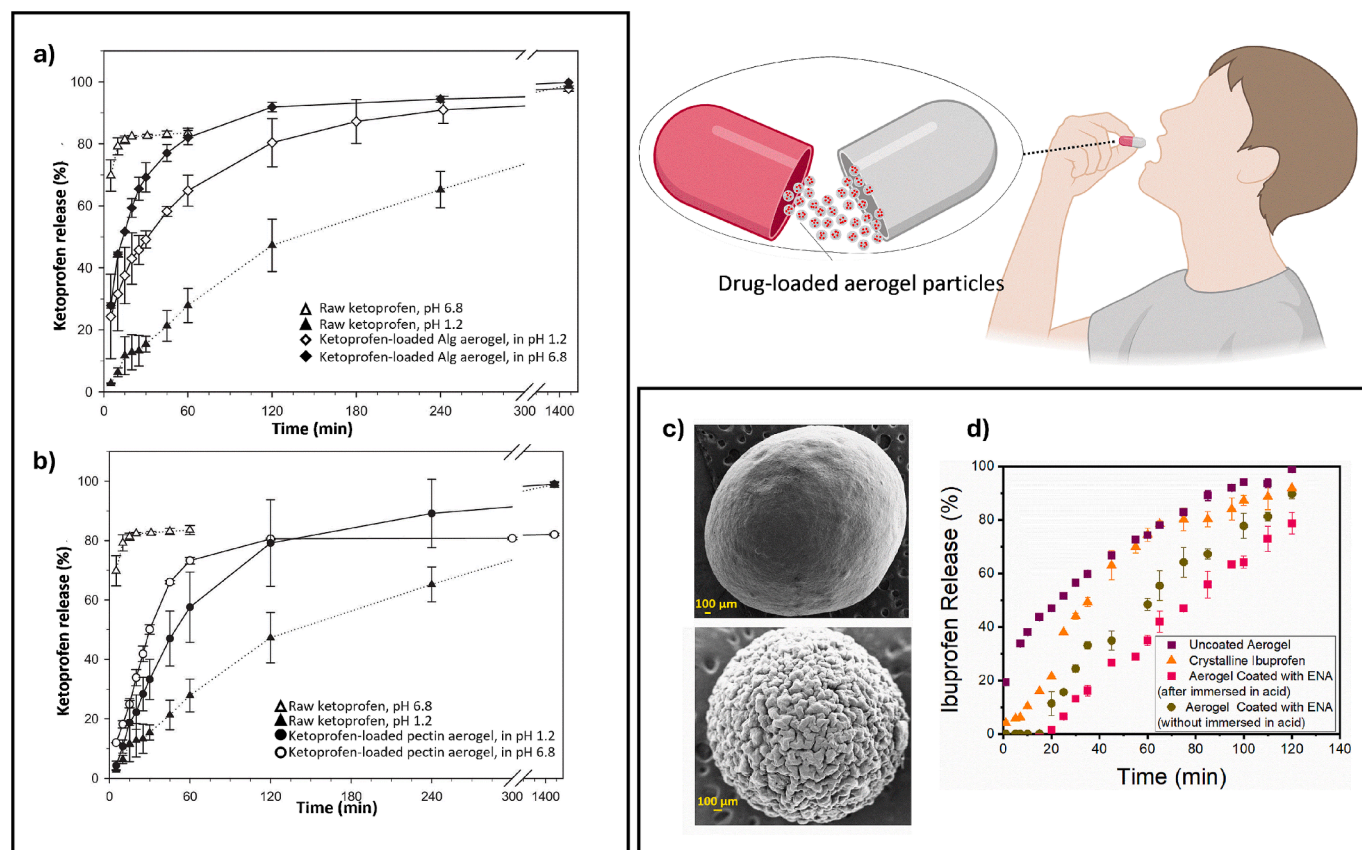


Fig. 9. Comparison of different *in vitro* drug release studies of aerogel particles for oral administration. For uncoated aerogels, (a) ketoprofen release from Alg particles under pH 1.2 and 6.8, and (b) ketoprofen release from pectin particles under pH 1.2 and 6.8 showed a sustained drug release, compared to raw ketoprofen. Adapted from (García-González et al., 2015) with permission. (c) For coated aerogel particles, (d) a delayed drug release was observed during the first 15 min, after increasing the pH from acidic conditions (pH 1.2) to neutral conditions (PBS pH 6.8), when compared to crystalline ibuprofen or uncoated formulations. Adapted from (Akgün et al., 2023) with permission.

conventional aerogels occurred in just 1 h (Pantić et al., 2020). In another example, hydrophilic and hydrophobic silica aerogel particles loaded with fluconazole were coated with PVA nanofibers (Afrashi et al., 2019). Fluconazole release rate from hydrophilic and hydrophobic silica aerogels increased by 3.7- and 2.5-fold, respectively, with respect to the crystalline drug form in a PBS solution. The uncoated aerogel powder exhibited a Fickian release mechanism, whereas the silica aerogel/PVA composites followed a non-Fickian mechanism, indicating a controlled release.

Coated aerogels were also successful in providing a pH-dependent release profile. Ibuprofen-loaded silica aerogel particles were coated with PEG and Eudragit® L via spray coating method and the release of the drug was evaluated in 0.1 M HCl and in PBS pH 7.2 media (Alnaief et al., 2012). The coating led to significant changes in the release rate of ibuprofen in acidic medium with less than 20 % of the loaded ibuprofen released from coated aerogels after 2 h, while almost 94 % of ibuprofen was released from the uncoated silica aerogels under the same conditions. At pH values above 5.5, Eudragit® L was soluble and the coating did not affect the release rate of ibuprofen in PBS pH 7.2 medium with a complete release of ibuprofen in less than 10 min.

Other polymers (trehalose, methacrylic acid-ethyl acrylate copolymer, dextran –Dex-, Alg) were also applied as coatings on aerogels to develop pH-responsive oral drug delivery systems. Curcumin release rate was studied for trehalose-coated starch aerogels via dip coating method in three different pH media (2.2, 5.5 and 7.4) (Izadi et al., 2023). In pH 2.2 medium, the release profile of curcumin from uncoated and coated aerogels was similar and ca. 80 % of drug was released within nearly 5 h. With increasing pH, curcumin release rate was reduced and 50 and 45 % of drug were released from coated aerogels in pH 5.5 and 7.4, respectively, within 8 h, while almost 70 % drug were released from uncoated aerogels for both pH and within the same time period. In another example, ibuprofen release in acidic medium was prevented via coating of Alg aerogels with a methacrylic acid-ethyl acrylate copolymer coating (CLT of 84.1 µm) in a Wurster fluidized bed (Fig. 9c) (Akgün et al., 2023). A slow ibuprofen release rate was achieved via the aerogel coating and only 13 % drug was released in 30 min in acidic medium, while 89 % of adsorbed ibuprofen was released in a basic medium after 2 h. 57 and 44 % of ibuprofen were released in 30 min from the uncoated aerogel counterpart and dissolved from the crystalline ibuprofen, respectively, in the acidic medium (Fig. 9d). Silica aerogels were coated with Dex and Dex aldehyde (Dex-CHO) for enzyme-triggered and colon-targeted 5-FU release via dip coating (Tiryaki et al., 2020). Release of 5-FU from uncoated silica aerogels was nearly 86 % for 24 h in simulated gastric, intestinal and colonic fluids. The drug release profiles from Dex and Dex-CHO coated silica aerogels in the gastric and intestinal fluids for 24 h were 1.7 and 3.4 %, respectively. In a stimulated colon tumour medium (acetate buffer with pH 5.5 and including dextranase enzyme), drug release from coated aerogels with Dex and Dex-CHO was recorded as 24.0 and 13.4 % for 24 h, respectively.

Alg core-shell aerogels fabricated by the prilling method also showed great potential as carriers for pH-dependent insulin release (Ozesme Taylan et al., 2025). Only 30 % of insulin was released in SGF after 120 min, whereas 60 % was released in SIF within the first hour, followed by a sustained release stage.

Multilayer coatings can also be used to tune the drug release profiles from aerogels. Coatings with several layers were applied to Alg aerogels loaded with nicotinic acid (Veronovski et al., 2013). The complete drug release was prolonged by increasing the number of Alg layers around the aerogels. 75 % of nicotinic acid was released in 5 min from uncoated aerogels, while only 50 % of nicotinic acid was released in 1 h from Alg aerogels coated with 8 layers. pH-sensitive and controlled drug release can be also obtained from aerogel particles with multilayer coatings (Aramideh et al., 2023). As an example, a multi-layered coating of chitosan (initial layer) and gelatin (outer layer) on silica aerogel particles significantly improved the controlled release of quercetin. Release studies at neutral (pH 7.4) and acidic (pH 5.6) conditions significantly

reduced the rapid initial drug release from the uncoated aerogels. Specifically, after 24 h in acidic conditions, 43 % of the drug was released from chitosan-coated aerogels, while only 27 % was released in the neutral medium. The addition of a gelatin outer layer further decreased the release in acidic conditions to 34 % within the same timeframe. Kinetic analysis indicated that the quercetin release from coated silica aerogels fitted to the Higuchi model, suggesting a diffusion-controlled release mechanism.

Initial research in oral drug delivery explored silica aerogels for their well-known sol-gel chemistry, however, their low biodegradability has limited their application in this field (Al-Najjar et al., 2021). Therefore, studies have shifted to biodegradable polymers such as alginate, starch, chitosan, and pectin. These biodegradable biopolymers are recognized as Generally Recognized As Safe (GRAS) by the US Food and Drug Administration (FDA) and demonstrated very promising results regarding sustained and pH-responsive drug release, site-specific delivery within the gastrointestinal tract, and protection of pH-sensitive drugs (Illanes-Bordomas et al., 2023; Mohammed et al., 2021). Moreover, they can undergo enzymatic or pH-triggered degradation in the gastrointestinal tract, therefore reducing the risk of long-term accumulation. Although particle size, surface characteristics, and dosage must be carefully controlled, the studies available so far generally report low *in vitro* cytotoxicity (Aramideh et al., 2023; Izadi et al., 2023). Alg is the most reported polysaccharide used for aerogel fabrication (Demina et al., 2024). Therefore, *in vivo* studies with calcium-crosslinked Alg aerogels have not reported significant adverse effects on liver or kidney function over short-term administration, and an increased abundance of some bacteria reported (Al-Najjar et al., 2021). Despite these promising findings, data on chronic exposure, effects on gut permeability, and interactions with the intestinal microbiota remain scarce, highlighting the need for further systematic *in vivo* and translational studies.

### 3.2. Skin drug delivery

The skin, the largest organ of the human body, performs several notable functions, including acting as physical barrier against pathogens, chemicals and other external damaging factors (Baker et al., 2023; Pei et al., 2023; Prausnitz et al., 2004). However, its integrity can be compromised by external factors, such as burns or wounds or even from pathological diseases (e.g., diabetic ulcers). The appropriate treatment of wounds and other skin disorders is essential to avoid further complications. Regarding wounds, it is important to consider the complexity associated with each specific wound and optimum dressings must ensure all the ideal treatment conditions, such as wound ventilation and exudate absorption (Bernardes et al., 2021). Additionally, dressings should be biodegradable, biocompatible, allow the complete wound covering, and adapt to different shapes and depths. An optimum wound dressing may also incorporate bioactive compounds to facilitate an accelerated optimal healing (Gorshkova et al., 2024).

Aerogels, in various sizes and forms (i.e. 3D-structures, and microparticles) have emerged as promising materials for a wide range of skin-related applications (transdermal drug delivery, dermatological therapies and also wound healing) (Croitoru et al., 2024). Beyond their inherent porosity and high specific surface area, aerogels have multiple advantages for wound healing. Notably, they exhibit excellent permeability for absorbing wound exudate and facilitating gas exchange. Moreover, their swelling behaviour under wet ambient is promising (Gorshkova et al., 2024). Once applied under a wound (Fig. 10a,b), aerogels can turn into a wet gel while remain in the aerogel form upon contact with the healthy and dry skin (Sellitto et al., 2023). Furthermore, aerogel microparticles in the powdered form can be directly applied to the wounds, cover them completely and adapt to different shapes including deep tissue cavities, thus enhancing their utility in clinical application (Bernardes et al., 2021).

Chitosan, alginate and pectin aerogel particles have shown promising results for wound care. Chitosan aerogel particles with few

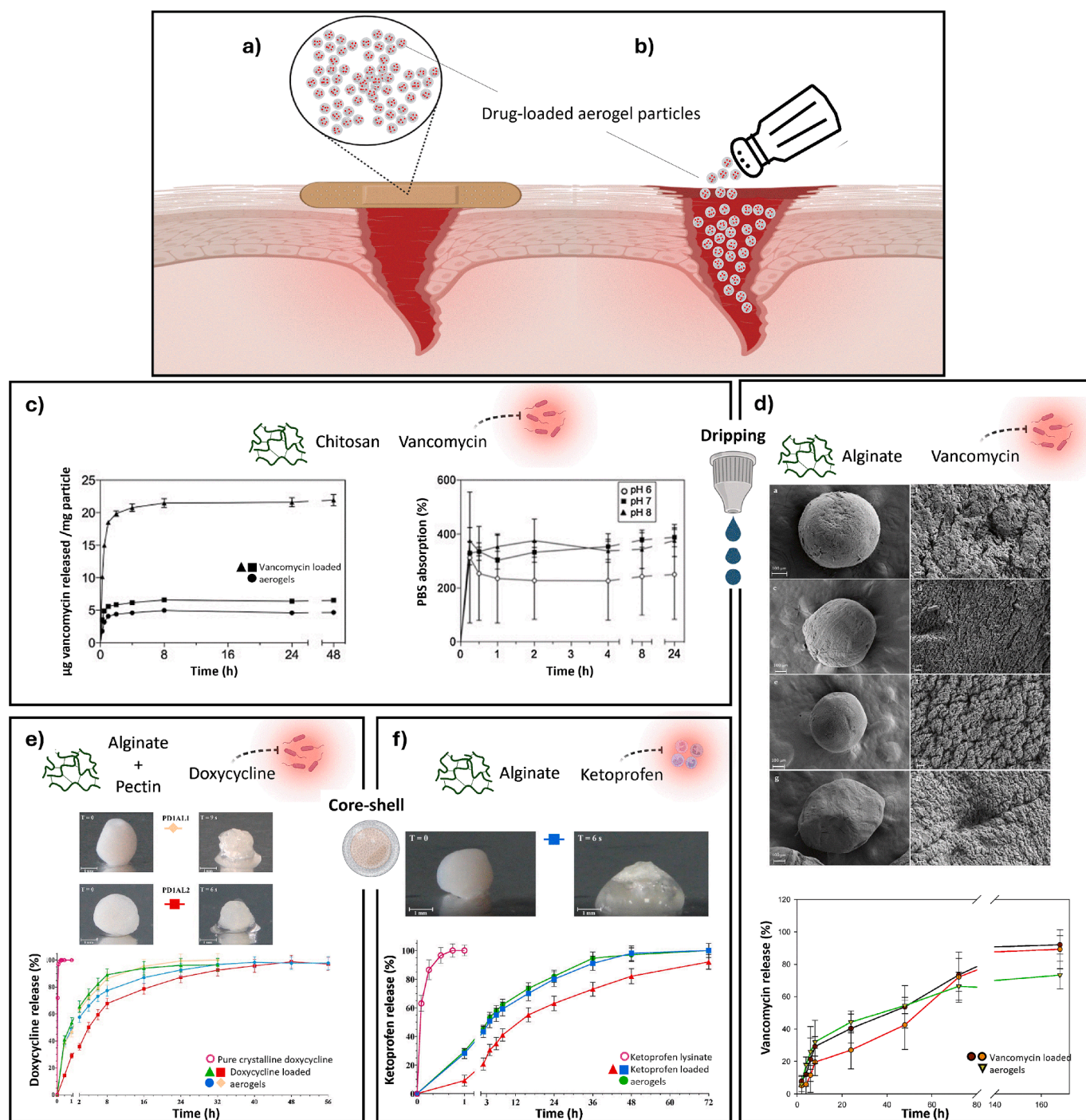


**Fig. 10.** Drug-loaded aerogel particles applied in wounds (a) in combination with dressings or (b) directly. Drug release profiles and fluid uptake of aerogel formulations: (c) Vancomycin-loaded chitosan aerogel particles (adapted from (López-Iglesias et al., 2019b) with permission), (d) vancomycin-loaded Alg aerogel particles (adapted from (Remuñán-Pose et al., 2022) with permission), (e) Doxycycline-loaded Alg/pectin (core-shell) aerogel particles (adapted from (De Cicco et al., 2016) with permission), and (f) ketoprofen-loaded Alg/Alg (core-shell) particles (adapted from (Sellitto et al., 2023) with permission).

millimetres (ca. 2–5 mm) were tested for hemostatic applications when applied directly to bleeding wounds (Lovskaya et al., 2020). Additionally, chitosan aerogels are particularly promising as drug carriers for wound care, once chitosan can also exhibit natural antimicrobial activity and ability to stimulate the tissue regeneration (Croitoru et al., 2024). As an example, chitosan aerogel particles with approximately 4 mm of diameter were engineered by dripping for the local delivery of vancomycin, a commonly used antibiotic for treating infected wounds (López-Iglesias et al., 2019b). Vancomycin hydrochloride was incorporated into a chitosan solution prior to gelation, and spherical particles

were obtained with a drug loading of  $27.3 \pm 2.8 \mu\text{g mg}^{-1}$ . Vancomycin was found to be distributed both adsorbed onto the porous matrix and chemically bound with the chitosan network, resulting in a two-phase release pattern: an initial burst followed by a sustained release over several hours (Fig. 10c). After just 2 h, vancomycin concentrations in the release medium exceeded the minimum inhibitory concentration (MIC) for *Staphylococcus aureus* ( $1\text{--}2 \mu\text{g mL}^{-1}$ ), the predominant pathogen in chronic wound infections. Although complete drug release was not achieved, the formulation maintained therapeutic levels over time, which is vital for preventing bacterial recolonization. These properties

make chitosan aerogels a compelling carrier option to offer prolonged drug release, high drug loading, and effective moisture and exudate management.

Alg aerogels particles have also shown strong potential in wound care due to their superabsorbent nature, especially under saline conditions. This is crucial for wound healing as Alg aerogels microparticles can simultaneously act as drug delivery systems and as effective absorbers of wound exudate (Mallepally et al., 2013). Vancomycin was successfully incorporated (loading of  $33.01 \pm 0.47 \mu\text{g mg}^{-1}$  with an encapsulation yield of 19.41 %) into Alg aerogels using an innovative approach based on DoD printing onto a superhydrophobic surface (Remuñán-Pose et al., 2022). In this case, vancomycin is known to interact electrostatically with Alg through the respective amino and carboxyl groups, which likely contributed to both the enhanced encapsulation efficiency and the controlled release behaviour. The aerogel particles exhibited a rapid drug release within the first 8 h, followed by a sustained release (Fig. 10d). MIC of vancomycin for *S. aureus* was achieved after the first 2 h, confirming the antimicrobial effectiveness of the formulation.

Another study engineered Alg aerogel particles by milling hydrogel monoliths and supplemented with calcium ( $\text{Ca}^{2+}$ ), zinc ( $\text{Zn}^{2+}$ ) and silver ( $\text{Ag}^+$ ) ions, with promising potential in wound care applications due to their ability to absorb fluids and to release bioactive ions beneficial to healing (Raman et al., 2019). While  $\text{Ca}^{2+}$  cations are commonly used to crosslink alginate, other divalent cations such as  $\text{Zn}^{2+}$  cation can also be employed. In the context of wound healing, both  $\text{Ca}^{2+}$  and  $\text{Zn}^{2+}$  cations play essential biological roles in the wound healing process.  $\text{Ca}^{2+}$  cations are involved in key phases such as blood clotting, inflammation, and tissue remodelling, while  $\text{Zn}^{2+}$  cation is crucial for immune function and cellular repair.  $\text{Ag}^+$  cations, on the other hand, are well known for their strong antimicrobial activity, making them valuable in wound care. Unlike  $\text{Ca}^{2+}$  cations, which remained throughout the solvent exchange and supercritical drying steps,  $\text{Zn}^{2+}$  cations significantly leached out of the gel during processing. However, the incorporation of  $\text{Ag}^+$  cations helped retain a higher amount of  $\text{Zn}^{2+}$  cations in the final aerogel formulation. When exposed to physiological buffers (HEPES-buffer pH 7.35), the Ca-alginate aerogel containing  $\text{Zn}^{2+}$  and  $\text{Ag}^+$  swelled significantly, absorbing large amounts of the liquid and releasing the ions.

Pectin, a highly hydrophilic polymer, shares similar absorption properties to Alg, making it valuable for developing wound care formulations (Munarin et al., 2012). An example combining Alg and pectin involved the use of coaxial printing to create core-shell aerogel particles loaded with doxycycline, an antimicrobial drug (De Cicco et al., 2016). The core consisted of amidated pectin containing doxycycline, while the shell was made of Alg. The core-shell particles had average diameters of ca. 3  $\mu\text{m}$ , where thicker alginate shells led to lower drug encapsulation efficiencies, likely due to an increased porosity in the outer layer. In contact with the wound fluid, these core-shell aerogel particles will swell and turn into a gel. Moreover, doxycycline in the core chemically interacted with pectin and Alg to provide a prolonged drug release, which can be extremely advantageous when combined it into dressings or gauzes (Fig. 10e).

Another advanced core-shell aerogel particles ( $\geq 1 \text{ mm}$ ) were developed to deliver ketoprofen lysinate, an anti-inflammatory drug, to treat wounds (Sellitto et al., 2023). In this case, the core consisted of an oil-in-water-in-oil emulsion containing the drug, and the shell was a thin Alg layer gelified with  $\text{CaCl}_2$ . The resulting drug-loaded core-shell particles underwent solvent exchange and were subsequently dried with  $\text{scCO}_2$  (40 °C, 140 bar for 270 min). During the  $\text{scCO}_2$  drying, the oily phase was removed without a significant drug loss. In addition to high drug loadings (encapsulation efficiency of 74 %), the aerogel particles displayed good textural properties, such as, high specific surface area (up to 417  $\text{m}^2 \text{g}^{-1}$ ) and porosity (up to 95 %), both crucial for wound treatment. Moreover, they formed a soft hydrogel within just 12 s upon contact with simulated wound fluid. The aerogels demonstrated strong fluid absorption capacity (505 %) and a prolonged release of ketoprofen

lysinate for up to 72 h (Fig. 10f). These core-shell Alg aerogels could serve as self-contained therapeutic systems, offering both sustained drug delivery and effective exudate management, particularly for acute and chronic wound care.

Overall, polysaccharide-based aerogels, particularly those derived from marine sources such as Alg and chitosan, have strong interest for skin-related applications especially in wound healing. This is largely due to their intrinsic physiological activity regarding antimicrobial and regenerative properties, that can be improved by the combination with bioactive compounds. Notably, several alginate-based dressings have already been successfully translated into clinical practice, where they mainly provide passive wound support through moisture regulation and infection control, supporting their favourable safety and biocompatibility profile. Building on this clinical foundation, current research is increasingly focused on the development of bioactive and multifunctional aerogel systems capable of actively promoting tissue regeneration through the incorporation of therapeutic agents (Mazurek et al., 2025). Nevertheless, despite their generally favourable biocompatibility profile, it should be noted that aerogel-based formulations may cause skin irritation or dryness in some cases (Boccia et al., 2023).

### 3.3. Pulmonary drug delivery

Lungs are a highly attractive route for drug administration due to their i) direct connection to the external environment, ii) close link to systemic circulation, iii) anatomical properties (large surface area, thin alveolar epithelium, rich vascularization) and iv) low enzymatic activity (García-González et al., 2021; Duong et al., 2021; Valente et al., 2022; Zhang et al., 2023). In addition, pulmonary delivery bypasses first-pass hepatic metabolism, minimizes systemic toxicity, and offers a non-invasive alternative to subcutaneous or intravenous injections (Hastedt et al., 2016). This allows both local and systemic delivery of therapeutic agents, with applications ranging from asthma treatment to gene therapy and vaccination (García-González et al., 2021; Duong et al., 2021; Zhang et al., 2023). To achieve therapeutic efficacy, inhaled formulations (i.e. particles containing the active compound) must be engineered for optimum lung deposition, with favourable aerodynamic properties, low density, and good flowability (Duong et al., 2021). Inhalable particles should have an aerodynamic diameter between 1 – 5  $\mu\text{m}$  for lung deposition, and less than 2  $\mu\text{m}$  to reach the alveoli (López-Iglesias et al., 2019a; Zhang et al., 2024). However, small particles are susceptible to clearance by alveolar macrophages. Therefore, large porous particles with low density, high sphericity and aerodynamic diameters in the 1 – 5  $\mu\text{m}$  range are ideal candidates for inhaled drug delivery (Duong et al., 2021).

Drug inhalation requires specialized devices (inhalers) that commonly generate aerosols, i.e. dispersions of solid or liquid particles in a gas. These include dry powder inhalers (DPIs) –for delivery of medication in the form of dry powder–, pressurized metered-dose inhalers (pMDIs), nebulizers and soft mist inhalers (SMIs) –for the delivery of aqueous solutions or suspensions in the aerosol– (Zhang et al., 2024). Among them, DPIs are the most suitable for solid formulations based on aerogel microparticles. Despite their widespread commercialization and use, conventional DPI formulations have limitations. They typically require high excipient-to-drug ratios to ensure dispersion and lung delivery, and also rely on fast-release formulations (Ke et al., 2022). For instance, BDP, a corticosteroid commonly used in the treatment for asthma, is currently marketed in DPIs (Fostair NEXThaler® 200  $\mu\text{g}/6 \mu\text{g}$ ) with formulations containing only 200  $\mu\text{g}$  of BDP and 6  $\mu\text{g}$  of formoterol fumarate dihydrate per 10 mg dose of inhalation powder, while lactose making up the remaining mass as excipient (Duong et al., 2024b; Chiesi Limited, 2019). This low drug loading in DPIs increases the inhaled powder burden, potentially reducing patient adherence. Aerogel microparticles with well-defined and preserved porosity, low density, high specific surface area, low aerodynamic diameter and high drug loading capacity represent a promising alternative recently explored for DPI

formulations (Table 3) (Duong et al., 2021). Alginate is one of the most promising polymers for producing aerogel particles suitable for pulmonary drug delivery. BDP-loaded Alg aerogel microparticles were produced through the emulsion-gelation process (particle diameter of ca. 2  $\mu\text{m}$ ) (Duong et al., 2024b) and by compressed air-assisted prilling gelation (particle diameter of ca. 38  $\mu\text{m}$ ) (Duong et al., 2024a), followed by scCO<sub>2</sub> drying. BDP were loaded into the aerogel particles via scCO<sub>2</sub> impregnation (65 °C, 215 bar) using acetone as a co-solvent to improve the drug solubility in the supercritical medium and facilitate its penetration into the aerogel structure. Using this strategy, a drug loading of ca. 5–7 wt% was achieved, being significantly higher contents than those in commercial DPIs formulations. The BDP-loaded Alg aerogel particles exhibited aerodynamic sizes below 5  $\mu\text{m}$ , suitable for deep lung deposition, as proven by *in vitro* aerosol deposition tests in a Next Generation Impactor (NGI) of the aerogel powder loaded into a DPI. *In vitro* release studies confirmed the controlled and sustained release behaviour of these aerogel formulations, showing an initial burst release followed by a prolonged release phase (Fig. 11a,b). *Ex vivo* studies using porcine lung tissue and Franz cells confirmed that BDP released from aerogels can permeate and be retained in bronchial tissues, highlighting the potential of BDP-loaded Alg aerogels as promising carriers for DPI formulations, with potential applications for asthmatic patients.

Salbutamol sulphate (SS), a bronchodilator widely used in inhaler devices for the management of asthma and chronic obstructive pulmonary disease, was incorporated for the first time into Alg aerogels produced by inkjet printing (López-Iglesias et al., 2019a). The resulting SS-loaded aerogel microparticles registered a drug loading of 3 wt%, a promising result considering that commercial SS dry powder inhalers typically deliver 50–100  $\mu\text{g}$  per dose. *In vitro* aerosol deposition tests using a DPI coupled to an NGI showed an excellent emitted dose for the total powder ( $97.5 \pm 1.2\%$ ) and a promising emitted dose of the drug itself ( $80.3 \pm 3.4\%$ ). The NGI results also showed that the aerogel microparticles are likely to deposit in the bronchi and bronchioles. SS release from aerogel particles exhibited an initial sudden release of ca. 10 %, followed by a controlled and sustained release over 10 h (Fig. 11c), an important feature that allow to reduce the administration frequency.

Systemic administration of drugs, including oral and intravenous routes, is still commonly used to treat several pulmonary disorders, including lung cancer. However, it often leads to undesired effects and may fail to achieve the desired therapeutic outcome. High drug doses are frequently required, increasing the risk of toxicity and, consequently, undesired secondary side effects. Inhalable formulations of these drugs

provide a promising strategy to improve local lung targeting and to reduce systemic exposure (Anderson et al., 2022). As an example, cisplatin, a chemotherapeutic drug, was successfully incorporated into Alg-chitosan aerogel microparticles prepared by the emulsion-gelation method (Alsmadi et al., 2020). Aerogels had a diameter of 0.43  $\mu\text{m}$ , specific surface area of 86  $\text{m}^2 \text{g}^{-1}$  and a mean mesopore size of 13.4 nm. Cisplatin was successfully impregnated with scCO<sub>2</sub> (drug loading > 76 %) within the aerogels' pores. No chemical interactions between the drug and the polymers took place, which contributed to a fast drug release within the first 2 h (ca. 60 %), followed by a sustained release over the following 6 h. This profile drastically contrasts from the fast dissolution of free cisplatin in less than 40 min. However, toxicity damage of the aerogel formulations was reported in mice after intratracheal administration and demands further studies.

Hydroxychloroquine (HCQ), a commonly orally administrated drug to treat malaria, was initially demonstrated (then retracted) promising potential for treating lung damage caused by infections such as COVID-19 (Gautret et al., 2025). Oral administration of HCQ exhibited secondary side effects and, therefore, the targeting of HCQ directly to the lungs was needed. HCQ was successfully incorporated into chitosan–Alg aerogel particles, produced via emulsion-gelation method, by drug impregnation during the scCO<sub>2</sub> drying process (40 °C, 200 bar) (Alsmadi et al., 2023). Aerogel microparticles had a drug loading of ca. 11 wt%. *In vitro* drug release studies revealed a controlled release profile for the HCQ-loaded aerogels. After 30 min, less than 50 % of the drug was released, whereas nearly 100 % of the free HCQ was dissolved. *In vivo* studies compared oral and intravenous administration of raw HCQ with intratracheal administration of the HCQ-loaded aerogel powder in rats. Intratracheal administration resulted in significantly higher lung accumulation, lower systemic exposure, and a prolonged lung retention time of approximately 98 h. This extended lung retention was partly attributed to the mucoadhesive properties of chitosan and Alg. The reduced systemic presence of HCQ reduced systemic side effects, such as cardiac arrhythmias and myocardial hypertrophy, making them a promising alternative to high oral doses for lung-affected conditions.

The presented studies on aerogel particles for pulmonary drug delivery have been focused on biocompatible and biodegradable polymers, with Alg being the most employed in this field, followed by chitosan. The safety of alginate particles for inhalation has been evaluated mainly due to the potential toxicity of residual Ca<sup>2+</sup> resulting from the cross-linking reaction (Chan and Mooney, 2013), however, *in vitro* cytotoxicity studies of CaCl<sub>2</sub>-crosslinked alginate aerogels using the NIH-3 T3 cell line report cell viability of approximately 80 %, which is considered

**Table 3**

Summary of engineered aerogel-based systems for pulmonary administration, including aerogel material source, preparation method, API, target disease, main features ( $d_p$  = particle diameter;  $A_{\text{BET}}$  = specific surface area;  $\Phi$  = porosity;  $d_{ae}$  = aerodynamic diameter), and the corresponding references. Notation: ns = not specified.

Aerogel material	Preparation methodology	API	Target Disease	Features				Ref.
				$d_p$ ( $\mu\text{m}$ )	$A_{\text{BET}}$ ( $\text{m}^2 \text{g}^{-1}$ )	$\Phi$ (%)	$d_{ae}$ ( $\mu\text{m}$ )	
Alginate	Emulsion gelation process followed by scCO <sub>2</sub> drying	Beclomethasone dipropionate (BDP)	Asthma	2.25	247 ± 12	90	1	(Duong et al., 2024b)
Alginate	Compressed air- assisted prilling gelation followed by scCO <sub>2</sub> drying	Beclomethasone dipropionate (BDP)	Asthma	38	351 ± 15	ns	1–5	(Duong et al., 2024a)
Alginate	Inkjet printing followed by scCO <sub>2</sub> drying	Salbutamol sulphate	Asthma and chronic obstructive pulmonary disease	23.8	180	97.7	2.4	(López-Iglesias et al., 2019a)
Alginate-hyaluronic acid	Emulsion gelation process followed by scCO <sub>2</sub> drying	Sodium naproxen	ns	< 34	354– 759	97.5 – 99.8	< 5	(Athamneh et al., 2019; Athamneh et al., 2021)
Chitosan-alginate	Emulsifying gelation method followed by scCO <sub>2</sub> drying	Hydroxychloroquine (HCQ)	COVID-19 (Retracted)	22.7	80	ns	1	(Alsmadi et al., 2023)
Chitosan-alginate	Emulsion gelation method followed by scCO <sub>2</sub> drying	Cisplatin	Lung Cancer	0.43	86	ns	ns	(Alsmadi et al., 2020)
Chitosan	Ionic gelation via dripping followed by scCO <sub>2</sub> drying	Salbutamol	ns	10	73–103	ns	ns	(Obaidat et al., 2015)

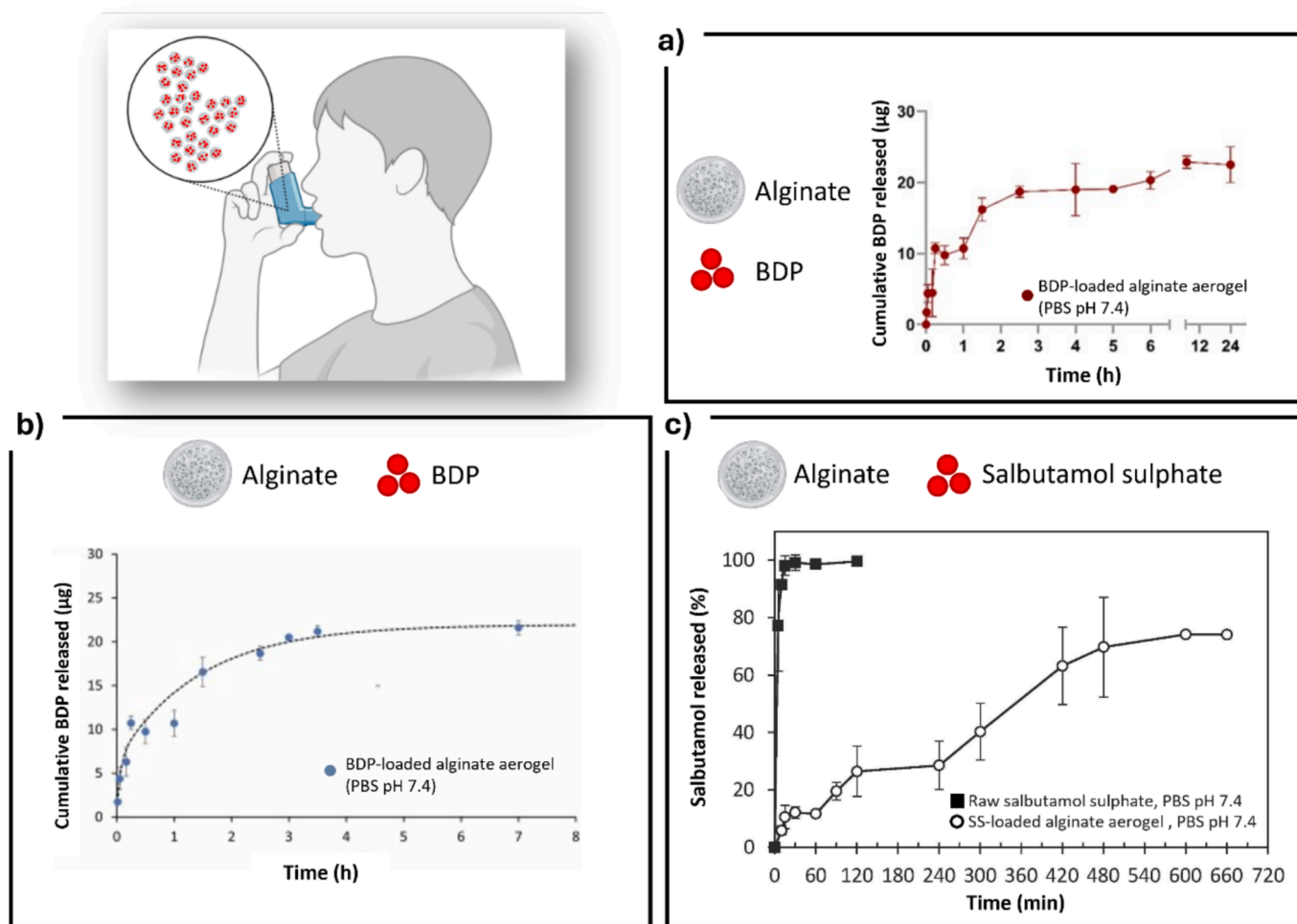


**Fig. 11.** *In vitro* drug release profiles of different aerogel particle formulations for pulmonary delivery. All formulations show an initial burst release of the drug followed by a slow and sustained release phase. The release profiles of (a,b) BDP from BDP-loaded alginate aerogels produced by compressed air-assisted prilling and by emulsion gelation, respectively, (adapted from (Duong et al., 2024a,b) with permission) and (c) salbutamol sulphate from salbutamol sulphate –loaded alginate aerogel (adapted from (López-Iglesias et al., 2019a) with permission).

non-cytotoxic according to ISO 10993 standards (Duong et al., 2024a). Additionally, it is also important to consider that Alg has been reported to increase mucus viscosity, which may aggravate mucus-related pathologies such as cystic fibrosis. Regarding chitosan, immunogenic responses occasionally associated with chitosan-based systems have been linked to residual allergenic contaminants, such as tropomyosin, rather than to chitosan itself (Valente et al., 2022). Despite the promising results on aerogel particles as inhalation drug delivery systems, the *in vivo* assessment of efficacy for inhaled formulations remains challenging due to the scarcity of validated animal models suitable for testing potential drug candidates in respiratory diseases (Anderson et al., 2022; Sécher et al., 2020). Moreover, although polysaccharide-based carriers offer clear advantages for pulmonary drug delivery, they have not yet progressed to clinical trial stages, highlighting the need for a comprehensive evaluation of their benefits and limitations before clinical translation (Valente et al., 2022).

#### 4. Challenges and future trends

Aerogel particles have evolved from a niche materials science curiosity into a highly promising platform for advanced biomedical applications. This transformation is driven by their unique properties, which allow for the precise engineering of particles with tuneable sizes, configurations, and shapes. The growing industrial interest in aerogel particle production is a testament to their value, as they facilitate the

definition of robust protocols to obtain reproducible batches and enable accurate dosing and blending with other materials. The ability to tune their size, shape, and surface chemistry unlocks an unprecedented control over drug loading, bioavailability, and release kinetics, positioning aerogel particles as a cornerstone of next-generation therapeutic designs.

Although these materials offer a versatile platform for biomedical applications, several multifaceted challenges hinder their immediate clinical translation (García-González et al., 2021). A primary obstacle to the large-scale adoption of aerogels in the pharmaceutical industry is the scalability and cost-effectiveness of the production process. Supercritical CO<sub>2</sub> drying, while unparalleled in preserving the delicate mesoporous network, remains a predominantly batchwise or semi-continuous process characterized by moderate-to-high capital and operational expenditures (Khuddeev et al., 2024). While pilot scale studies have demonstrated the feasibility of using autoclaves up to 100 L, further engineering of robust fully continuous drying platforms is still required to achieve the throughput needed to meet global pharmaceutical production demands (De Marco et al., 2018; Ruiz and Cavier, 2018; Manke et al., 2026). The manufacturing of aerogel particles under Good Manufacturing Practices (GMP) also needs to be implemented particularly for the supercritical drying step, but it seems feasible in a rather straightforward way as GMP-compliant supercritical equipment is already existing and installed worldwide in pharmaceutical plants and available from several technological suppliers. Beyond manufacturing,

the mechanical robustness of aerogel particles remains a significant concern for industrial handling. Their inherent fragility often leads to dusting or structural collapse during processes like tableting, which can compromise dosage precision and requires specific measures for a safe personnel handling (Boccia et al., 2023; Vareda et al., 2021). Furthermore, the hygroscopic nature of biopolymer-based aerogels may necessitate advanced moisture-protective packaging to prevent pore shrinkage upon a long-term storage, and to maintain the stability of the encapsulated payload over its shelf life.

Beyond manufacturing constraints, regulatory compliance and stringent sterility standards present significant hurdles. For biomedical applications, particularly via pulmonary and parenteral routes, maintaining sterility throughout the multi-step sequence of sol-gel synthesis, solvent exchange, and supercritical drying is exceedingly complex. Conventional sterilization techniques, such as autoclaving or gamma irradiation, often compromise the fragile aerogel framework or inadvertently alter its surface chemistry (Carracedo-Pérez et al., 2024). Consequently, scCO<sub>2</sub> has already been successfully applied for sterilization of starch and alginate aerogels, effectively preserving their structural integrity (Carracedo-Pérez et al., 2024; Carracedo-Pérez et al., 2026). Furthermore, the long-term metabolic fate and biostability of aerogel particles must be thoroughly addressed. The long-term impact of persistent aerogel fragments within the lung parenchyma or systemic circulation demands comprehensive *in vivo* toxicological profiling that extends beyond current short-term experimental models (Verma et al., 2024).

Future research trends are increasingly focused on addressing these obstacles through the development of smart, multifunctional, personalized and sustainable systems. The field is moving toward the functionalization of aerogel surfaces with stimuli-responsive polymers that trigger drug release in response to specific physiological cues, such as pH fluctuations in the tumor microenvironment or enzymatic activity in the gastrointestinal tract (Chen et al., 2026). Concurrently, the migration of innovative techniques like atomic layer deposition and cold plasma coating into the biomedical sector enables nanometric control over internal pore surfaces (Baumann et al., 2006; Schroeter et al., 2021b). Besides, the use of Artificial Intelligence (AI)/Machine Learning tools in aerogel research can significantly reduce trial-and-error in the laboratory and optimize the synthesis parameters such as precursor concentration, pH, and drying conditions to achieve design-on-demand aerogel particles with pre-defined release profiles (Owusu et al., 2025). These methods offer a promising pathway to enhance stability and provide an additional layer of control over release kinetics without sacrificing the core porosity. Additionally, the integration of aerogel technology with 3D printing facilitates the fabrication of patient-specific dosage forms, aligning the field with the emerging paradigm of precision medicine (Iglesias-Mejuto and García-González, 2022). Aerogels can be utilized in bio-inks or as sacrificial templates (Okkabaz et al., 2026) to create complex, vascularized tissue scaffolds able to mimic the extracellular matrix. This integration paves the way for personalized medicine, where patient-specific implants or inhalable microparticles are tailored to an individual's genetic and physiological profile. Finally, the shift toward green chemistry and circular economy will drive the development of sustainable aerogel production (García-González et al., 2025). Future research will prioritize the use of agro-industrial waste and renewable biopolymers, combined with solvent-free or supercritical-assisted recycling methods, to minimize the environmental footprint of aerogel manufacturing.

Ultimately, while the path to clinical implementation is characterized by technical and regulatory challenges, the evolution of scalable manufacturing and a deeper understanding of material-biological interactions will eventually enable aerogel particles to serve as advanced systems for the most complex therapeutic needs.

## 5. Conclusions

The comprehensive analysis presented in this review confirms that aerogel particles are high-performance solutions for the most demanding challenges in modern medicine using the currently available production technologies. Their emergence as a cornerstone of next-generation drug delivery is underpinned by their extraordinary structural properties, specifically their hierarchical porosity and vast internal surface area, which provide an unparalleled degree of control over the spatial and temporal release of diverse payloads.

One of the most significant conclusions drawn from recent advancements is the clear superiority of the particulate form over traditional monolithic aerogels in clinical and industrial contexts. The engineering of aerogels into discrete, spherical micro-particles has effectively bridged the gap between laboratory scale synthesis and pharmaceutical manufacturing. The optimization of particle morphology allows researchers to successfully address critical bottlenecks such as dose uniformity, flowability, and the precise control of aerodynamic diameters, which are essential for the reproducibility required by global regulatory standards. Moreover, the inherent flexibility of the sol-gel process, coupled with innovative supercritical drying techniques, allows for the encapsulation of a wide spectrum of therapeutic agents ranging from small hydrophobic molecules to sensitive biopharmaceuticals like proteins and nucleic acids without compromising their biological activity.

As the field moves toward commercial reality, the focus must shift from basic feasibility to the nuances of material-biological interactions and advanced manufacturing logic. The structural biomimicry of aerogel particles, which closely resembles the natural extracellular matrix, opens extraordinary avenues in regenerative medicine. Their potential to act simultaneously as a physical scaffold and a biochemical signalling centre positions them as a unique tool for tissue engineering and personalized implants. Yet, this potential can only be fully realized by overcoming the remaining hurdles of long-term biostability and the metabolic fate of aerogel fragments within the human body. The development of standardized toxicological profiles and comprehensive *in vivo* clearance studies remains a mandatory prerequisite for the next phase of clinical trials.

Looking at the broader perspective, the integration of aerogel particles into the modern biomedical portfolio requires a holistic approach that harmonizes scalable green production with stringent sterility requirements. The move toward sterile-by-design processes and the utilization of agro-industrial waste for biopolymer precursors reflect a maturing field that is increasingly conscious of both clinical safety and environmental sustainability. These efforts, combined with the emerging digital transformation through AI of material science, ensure that aerogels are not just a temporary trend but a permanent fixture in the future of healthcare.

In summary, aerogel particles stand at a critical juncture of innovation, representing a rare synergy where superior material properties meet delicate clinical needs. Interdisciplinary collaborations between chemists, engineers, life scientists and clinicians continue to deepen, so that obstacles that currently hinder their widespread adoption are being steadily dismantled. Ultimately, aerogel-based systems are poised to redefine the standards of precision medicine, evolving into smart, responsive, and life-saving tools that will fundamentally enhance the efficacy of complex therapeutic interventions in the decades to come.

## Funding sources

This work was funded by MICIU [PID2023-151340OB-I00/AEI/10.13039/501100011033], Xunta de Galicia [ED431C 2024/009], Agencia Estatal de Investigación [AEI], GAIN [Vinnovate call, AERO-CARE, IN848G 2024/01] and ERDF/EU funds. This work was carried out within the framework of the ECOAeroGELS COST Innovators' Grant (ref. IG18125) funded by the European Commission. S.M.G. and C.I.-B.

acknowledge MCINN and FSE + for their FPI fellowships [PREP2023-000885/AEI/10.13039/501100011033] and [PRE2021-097177/AEI/10.13039/501100011033], respectively.

### CRedit authorship contribution statement

**Susana M. Gomes:** Writing – review & editing, Writing – original draft, Visualization, Methodology, Investigation, Conceptualization. **Carlos Illanes-Bordomás:** Writing – review & editing, Writing – original draft, Investigation. **Carlos A. García-González:** Writing – review & editing, Writing – original draft, Methodology, Investigation, Conceptualization. **Işık Sena Akgün:** Writing – review & editing, Writing – original draft, Methodology, Investigation, Conceptualization.

### Declaration of competing interest

The authors declare that they have no known competing financial interests or personal relationships that could have appeared to influence the work reported in this paper.

### Acknowledgments

This work was funded by MICIU [PID2023-151340OB-I00/AEI/10.13039/501100011033], Xunta de Galicia [ED431C 2024/009], Agencia Estatal de Investigación [AEI], GAIN [Vinnovate call, AERO-CARE, IN848G 2024/01] and ERDF/EU funds. This work was carried out within the framework of the ECOAEROGELS COST Innovators' Grant (ref. IG18125) funded by the European Commission. S.M.G. and C.I.-B. acknowledge MCINN and FSE+ for their FPI fellowships [PREP2023-000885/AEI/10.13039/501100011033] and [PRE2021-097177/AEI/10.13039/501100011033], respectively.

### Data availability

Data will be made available on request.

### References

- Abdul Halim, Z.A., Mat Yajid, M.A., Idris, M.H., Hamdan, H., 2018. Physicochemical and thermal properties of silica Aerogel–Poly vinyl alcohol / Core-Shell structure prepared using fluidized bed coating process for thermal insulation applications. *Mater. Chem. Phys.* 215, 269–276. <https://doi.org/10.1016/j.matchemphys.2018.05.019>.
- Afrashi, M., Semnani, D., Talebi, Z., Dehghan, P., Maheronnaghsh, M., 2019. Novel multi-layer silica aerogel/PVA composite for controlled drug delivery. *Mater. Res. Express* 6, 095408. <https://doi.org/10.1088/2053-1591/ab3097>.
- Akgün, I.S., Demir, E., Işık, M., Ekmekçiyan, N., Şenses, E., Erkey, C., 2022. Protective coating of highly porous alginate aerogel particles in a Wurster fluidized bed. *Powder Technol.* 402, 117331. <https://doi.org/10.1016/j.powtec.2022.117331>.
- Akgün, I.S., Erkey, C., 2019. Investigation of hydrodynamic behavior of alginate aerogel particles in a laboratory scale wurster fluidized bed. *Molecules* 24, 2915. <https://doi.org/10.3390/molecules24162915>.
- Akgün, I.S., Erkey, C., 2021. Fluidization regimes for alginate aerogel particles in a laboratory scale Wurster fluidized bed. *Powder Technol.* 387, 295–312. <https://doi.org/10.1016/j.powtec.2021.04.007>.
- Akgün, I.S., Ulker, Z., Demir, E., Işık, M., Ekmekçiyan, N., Darvishi, S., et al., 2023. Enteric coating of drug loaded aerogel particles in a wurster fluidized bed and its effect on release behaviour. *J Drug Deliv Sci Technol* 82, 104279. <https://doi.org/10.1016/j.jddst.2023.104279>.
- Alnaief, M., Alzaitoun, M.A., García-González, C.A., Smirnova, I., 2011. Preparation of biodegradable nanoporous microspherical aerogel based on alginate. *Carbohydr. Polym.* 84, 1011–1018. <https://doi.org/10.1016/j.carbpol.2010.12.060>.
- Alnaief, M., Antonyuk, S., Hentzschel, C.M., Leopold, C.S., Heinrich, S., Smirnova, I., 2012. A novel process for coating of silica aerogel microspheres for controlled drug release applications. *Microporous Mesoporous Mater.* 160, 167–173. <https://doi.org/10.1016/j.micromeso.2012.02.009>.
- Al-Naijar, M.A.A., Athamneh, T., AbuTayeh, R., Bashedi, I., Leopold, C., Gurikov, P., et al., 2021. Evaluation of the orally administered calcium alginate aerogel on the changes of gut microbiota and hepatic and renal function of Wistar rats. *PLoS One* 16, e0247633. <https://doi.org/10.1371/journal.pone.0247633>.
- Alqahtani, M.S., Kazi, M., Alsenaidy, M.A., Ahmad, M.Z., 2021. Advances in oral drug delivery. *Front. Pharmacol.* 12, 618411. <https://doi.org/10.3389/fphar.2021.618411>.
- Alsmadi, M.M., Obaidat, R.M., Alnaief, M., Albiss, B.A., Hailat, N., 2020. Development, in vitro characterization, and in vivo toxicity evaluation of chitosan-alginate nanoporous carriers loaded with cisplatin for lung cancer treatment. *AAPS PharmSciTech* 21. <https://doi.org/10.1208/s12249-020-01735-8>.
- Alsmadi, M.M., Jaradat, M.M., Obaidat, R.M., Alnaief, M., Tayyem, R., Idkaidek, N., 2023. The in vitro, in vivo, and PBPK evaluation of a novel lung-targeted cardiac-safe hydroxychloroquine inhalation aerogel. *AAPS PharmSciTech* 24. <https://doi.org/10.1208/s12249-023-02627-3>.
- Anderson, S., Atkins, P., Bäckman, P., Cipolla, D., Clark, A., Daviskas, E., et al., 2022. Inhaled medicines: past, present, and future. *Pharmacol. Rev.* 74, 48–118. <https://doi.org/10.1124/pharmrev.120.000108>.
- Antonyuk, S., Heinrich, S., Smirnova, I., 2012. Discrete element study of aerogel particle dynamics in a spouted bed apparatus. *Chem. Eng. Technol.* 35, 1427–1434. <https://doi.org/10.1002/ceat.201200083>.
- Antonyuk, S., Heinrich, S., Gurikov, P., Raman, S., Smirnova, I., 2015. Influence of coating and wetting on the mechanical behaviour of highly porous cylindrical aerogel particles. *Powder Technol.* 285, 34–43. <https://doi.org/10.1016/j.powtec.2015.05.004>.
- Aramideh, A., Ashjari, M., Niazi, Z., 2023. Effects of natural polymers for enhanced silica-based mesoporous drug carrier. *J. Drug. Deliv. Sci. Technol.* 81, 104189. <https://doi.org/10.1016/j.jddst.2023.104189>.
- Athamneh, T., Amin, A., Benke, E., Ambrus, R., Leopold, C.S., Gurikov, P., et al., 2019. Alginate and hybrid alginate-hyaluronic acid aerogel microspheres as potential carrier for pulmonary drug delivery. *J. Supercrit. Fluids* 150, 49–55. <https://doi.org/10.1016/j.supflu.2019.04.013>.
- Athamneh, T., Amin, A., Benke, E., Ambrus, R., Gurikov, P., Smirnova, I., et al., 2021. Pulmonary drug delivery with aerogels: engineering of alginate and alginate-hyaluronic acid microspheres. *Pharm. Dev. Technol.* 26, 509–521. <https://doi.org/10.1080/10837450.2021.1888979>.
- Auriemma, G., Russo, P., Del Gaudio, P., García-González, C.A., Landín, M., Aquino, R.P., 2020. Technologies and formulation design of polysaccharide-based hydrogels for drug delivery. *Molecules* 25, 3156. <https://doi.org/10.3390/molecules25143156>.
- Auriemma, G., Cerciello, A., Aquino, R.P., Del Gaudio, P., Fusco, B.M., Russo, P., 2020. Pectin and zinc alginate: the right inner/outer polymer combination for core-shell drug delivery systems. *Pharmaceutics* 12, 87. <https://doi.org/10.3390/pharmaceutics12020087>.
- Baker, P., Huang, C., Radi, R., Moll, S.B., Jules, E., Arbiser, J.L., 2023. Skin barrier function: the interplay of physical, chemical, and immunologic properties. *Cells* 12, 2745. <https://doi.org/10.3390/cells12232745>.
- Baumann, T.F., Biener, J., Wang, Y.M., Kucheyev, S.O., Nelson, E.J., Satcher, J.H., et al., 2006. Atomic layer deposition of uniform metal coatings on highly porous aerogel substrates. *Chem. Mater.* 18, 6106–6108. <https://doi.org/10.1021/cm061752g>.
- Bernardes, B.G., Del Gaudio, P., Alves, P., Costa, R., García-González, C.A., Oliveira, A.L., 2021. Bioaerogels: promising nanostructured materials in fluid management, healing and regeneration of wounds. *Molecules* 26, 3834. <https://doi.org/10.3390/molecules26133834>.
- Betz, M., García-González, C.A., Subrahmanyam, R.P., Smirnova, I., Kulozik, U., 2012. Preparation of novel whey protein-based aerogels as drug carriers for life science applications. *J. Supercrit. Fluids* 72, 111–119. <https://doi.org/10.1016/j.supflu.2012.08.019>.
- Boccia, A.C., Pulvirenti, A., García-González, C.A., Grisi, F., Neagu, M., 2023. Compendium of safety regulatory for safe applications of aerogels. *Gels* 9, 842. <https://doi.org/10.3390/gels9110842>.
- Bordón, M.G., Alasino, N.P.X., Villanueva-Lazo, Á., Carrera-Sánchez, C., Pedroche-Jiménez, J., Millán-Linares, M.D.C., et al., 2021. Scale-up and optimization of the spray drying conditions for the development of functional microparticles based on chia oil. *Food Bioprod. Process.* 130, 48–67. <https://doi.org/10.1016/j.fbp.2021.08.006>.
- Brandenberger, H., Widmer, F., 1998. A new multinozzle encapsulation/immobilisation system to produce uniform beads of alginate. *J. Biotechnol.* 63, 73–80. [https://doi.org/10.1016/s0168-1656\(98\)00077-7](https://doi.org/10.1016/s0168-1656(98)00077-7).
- Bugnone, C.A., Ronchetti, S., Manna, L., Bancho, M., 2018. An emulsification/internal setting technique for the preparation of coated and uncoated hybrid silica/alginate aerogel beads for controlled drug delivery. *J. Supercrit. Fluids* 142, 1–9. <https://doi.org/10.1016/j.supflu.2018.07.007>.
- Cai, G., Ni, H., Li, X., Wang, Y., Zhao, H., 2023. Eco-friendly fabrication of highly stable silica aerogel microspheres with core-shell structure. *Polymers* 15, 1882. <https://doi.org/10.3390/polym15081882>.
- Carracedo-Pérez, M., Ardao, I., López-Iglesias, C., Magariños, B., García-González, C.A., 2024. Direct and green production of sterile aerogels using supercritical fluid technology for biomedical applications. *J. CO2 Util.* 86, 102891. <https://doi.org/10.1016/j.jcou.2024.102891>.
- Carracedo-Pérez, M., Boccia, A.C., Ardao, I., Passos, C.P., Santos-Rosales, V., Santos, B., et al., 2026. Engineering of green sterilization technology to obtain biocompatible aerogels: supercritical CO<sub>2</sub> versus ethylene oxide and gamma radiation. *Biomater. Adv.* 182, 214698. <https://doi.org/10.1016/j.bioadv.2025.214698>.
- Carrêlo, H., Cidade, M.T., Borges, J.P., Soares, P., 2023. Gellan gum/alginate microparticles as drug delivery vehicles: DOE production optimization and drug delivery. *Pharmaceutics* 16, 1029. <https://doi.org/10.3390/ph16071029>.
- Cerciello, A., Auriemma, G., Morello, S., Pinto, A., Del Gaudio, P., Russo, P., et al., 2015. Design and in vivo anti-inflammatory effect of ketoprofen delayed delivery systems. *J. Pharm. Sci.* 104, 3451–3458. <https://doi.org/10.1002/jps.24554>.
- Chan, G., Mooney, D.J., 2013. Ca<sup>2+</sup> released from calcium alginate gels can promote inflammatory responses in vitro and in vivo. *Acta Biomater.* 9, 9281–9291. <https://doi.org/10.1016/j.actbio.2013.08.002>.

- Chen, J., Wang, Y., Gong, M., Wang, D., Lu, J., Chen, L., et al., 2026. A review of  $\beta$ -lactoglobulin-based biomaterials: From structural engineering to multifunctional biomedical applications. *Adv. Funct. Mater.* 27338. <https://doi.org/10.1002/adfm.202527338>.
- Ching, S.H., Bansal, N., Bhandari, B., 2017. Alginate gel particles—A review of production techniques and physical properties. *Crit. Rev. Food Sci. Nutr.* 57, 1133–1152. <https://doi.org/10.1080/10408398.2014.965773>.
- Croitoru, G.-A., Pîrvulescu, D.-C., Niculescu, A.-G., Rădulescu, M., Grumezescu, A.M., Nicolae, C.-L., 2024. Advancements in aerogel technology for antimicrobial therapy: A review. *Nanomaterials* 14, 1110. <https://doi.org/10.3390/nano14131110>.
- Cui, J.-H., Goh, J.-S., Park, S.-Y., Kim, P.-H., Lee, B.-J., 2001. Preparation and physical characterization of alginate microparticles using air atomization method. *Drug Dev. Ind. Pharm.* 27, 309–319. <https://doi.org/10.1081/DDC-100103730>.
- De Cicco, F., Russo, P., Reverchon, E., García-González, C.A., Aquino, R.P., Del Gaudio, P., 2016. Prilling and supercritical drying: A successful duo to produce core-shell polysaccharide aerogel beads for wound healing. *Carbohydr. Polym.* 147, 482–489. <https://doi.org/10.1016/j.carbpol.2016.04.031>.
- de Gans, B.-J., Duineveld, P.C., Schubert, U.S., 2004. Inkjet printing of polymers: State of the art and future developments. *Adv. Mater.* 16, 203–213. <https://doi.org/10.1002/adma.200300385>.
- De Marco, I., Iannone, R., Miranda, S., Riemma, S., 2018. An environmental study on starch aerogel for drug delivery applications: Effect of plant scale-up. *Int. J. Life Cycle Assess.* 23, 1228–1239. <https://doi.org/10.1007/s11367-017-1351-6>.
- Demina, T.S., Minaev, N.V., Akopova, T.A., 2024. Polysaccharide-based aerogels fabricated via supercritical fluid drying: A systematic review. *Polym. Bull.* 81, 13331–13356. <https://doi.org/10.1007/s00289-024-05359-x>.
- Dervin, S., Pillai, S.C., 2017. An Introduction to Sol-Gel Processing for Aerogels. In: Pillai, S.C., Behir, S. (Eds.), *Sol-Gel Mater. Energy Environ. Electron. Appl.* Springer International Publishing, Cham, pp. 1–22. [https://doi.org/10.1007/978-3-319-51044-4\\_1](https://doi.org/10.1007/978-3-319-51044-4_1).
- Doméjean, H., La Motte, D.e., Saint Pierre, M., Funfak, A., Atrux-Tallau, N., Alessandri, K., Nassoy, P., et al., 2017. Controlled production of sub-millimeter liquid core hydrogel capsules for parallelized 3D cell culture. *Lab Chip* 17, 110–119. <https://doi.org/10.1039/C6LC00848H>.
- Duong, T., López-Iglesias, C., Bianchera, A., Vivero-Lopez, M., Ardao, I., Bettini, R., et al., 2024b. Green CO<sub>2</sub> technology for the preparation of aerogel dry powder loaded with beclomethasone dipropionate. *J. CO<sub>2</sub> Util.* 81, 102722. <https://doi.org/10.1016/j.jcou.2024.102722>.
- Duong, T., López-Iglesias, C., Szweczyk, P.K., Stachewicz, U., Barros, J., Alvarez-Lorenzo, C., et al., 2021. A pathway from porous particle technology toward tailoring aerogels for pulmonary drug administration. *Front. Bioeng. Biotechnol.* 9, 671381. <https://doi.org/10.3389/fbioe.2021.671381>.
- Duong, T., Vivero-Lopez, M., Ardao, I., Alvarez-Lorenzo, C., Forgács, A., Kalmár, J., et al., 2024a. Alginate aerogels by spray gelation for enhanced pulmonary delivery and solubilization of beclomethasone dipropionate. *Chem. Eng. J.* 485, 149849. <https://doi.org/10.1016/j.cej.2024.149849>.
- Erkey, C., 2009. Preparation of metallic supported nanoparticles and films using supercritical fluid deposition. *J. Supercrit. Fluids* 47, 517–522. <https://doi.org/10.1016/j.supflu.2008.10.019>.
- Eslamian, M., Ashgriz, N., 2011. Drop-on-Demand Drop Generators. *Sprays*, Boston, MA, USA, pp. 581–601. [https://doi.org/10.1007/978-1-4419-7264-4\\_25](https://doi.org/10.1007/978-1-4419-7264-4_25).
- Feng, J., Ma, Z., Wu, J., Zhou, Z., Liu, Z., Hou, B., et al., 2025. Fire-safe aerogels and foams for thermal insulation: from materials to properties. *Adv. Mater.* 37. <https://doi.org/10.1002/adma.202411856>.
- Ganesan, K., Budtova, T., Ratke, L., Gurikov, P., Baudron, V., Preibisch, I., et al., 2018. Review on the production of polysaccharide aerogel particles. *Materials* 11, 2144. <https://doi.org/10.3390/ma1112144>.
- García-González, C.A., Smirnova, I., 2013. Use of supercritical fluid technology for the production of tailor-made aerogel particles for delivery systems. *J. Supercrit. Fluids* 79, 152–158. <https://doi.org/10.1016/j.supflu.2013.03.001>.
- García-González, C.A., Alnaief, M., Smirnova, I., 2011. Polysaccharide-based aerogels—promising biodegradable carriers for drug delivery systems. *Carbohydr. Polym.* 86, 1425–1438. <https://doi.org/10.1016/j.carbpol.2011.06.066>.
- García-González, C.A., Uy, J.J., Alnaief, M., Smirnova, I., 2012. Preparation of tailor-made starch-based aerogel microspheres by the emulsion-gelation method. *Carbohydr. Polym.* 88, 1378–1386. <https://doi.org/10.1016/j.carbpol.2012.02.023>.
- García-González, C.A., Jin, M., Gerth, J., Alvarez-Lorenzo, C., Smirnova, I., 2015. Polysaccharide-based aerogel microspheres for oral drug delivery. *Carbohydr. Polym.* 117, 797–806. <https://doi.org/10.1016/j.carbpol.2014.10.045>.
- García-González, C.A., Sosnik, A., Kalmár, J., De Marco, I., Erkey, C., Concheiro, A., et al., 2021. Aerogels in drug delivery: From design to application. *J. Control. Release* 332, 40–63. <https://doi.org/10.1016/j.jconrel.2021.02.012>.
- García-González, C.A., Blanco-Vales, M., Barros, J., Boccia, A.C., Budtova, T., Durães, L., et al., 2025. Review and perspectives on the sustainability of organic aerogels. *ACS Sustain. Chem. Eng.* 13, 6469–6492. <https://doi.org/10.1021/acssuschemeng.4c09747>.
- Gautret, P., Lagier, J.-C., Parola, P., Hoang, V.T., Meddeb, L., Mailhe, M., et al., 2025. Retraction notice to “Hydroxychloroquine and azithromycin as a treatment of COVID-19: results of an open-label non-randomized clinical trial” [International Journal of Antimicrobial Agents 56 (2020), 105949]. *Int. J. Antimicrob. Agents* 65, 107416. <https://doi.org/10.1016/j.ijantimicag.2024.107416>.
- Giray, S., Bal, T., Kartal, A.M., Kizilel, S., Erkey, C., 2012. Controlled drug delivery through a novel PEG hydrogel encapsulated silica aerogel system. *J. Biomed. Mater. Res. A* 100A, 1307–1315. <https://doi.org/10.1002/jbm.a.34056>.
- Gorshkova, N.A., Brovko, O.S., Palamarchuk, I.A., Ivahnov, A.D., Bogdanovich, N.I., Vorob'eva, T.Ya., 2024. Preparation of an Antibacterial Composite Aerogel for Biomedical Purposes Based on an Alginate–Chitosan Complex and Calcium Carbonate. *Appl. Biochem. Microbiol.* 60, 194–200. <https://doi.org/10.1134/S0003683824020042>.
- Goslinka, M., Selmer, I., Kleemann, C., Kulozik, U., Smirnova, I., Heinrich, S., 2019. Novel technique for measurement of coating layer thickness of fine and porous particles using focused ion beam. *Particuology* 42, 190–198. <https://doi.org/10.1016/j.partic.2018.03.002>.
- Hastedt, J.E., Bäckman, P., Clark, A.R., Doub, W., Hickey, A., Hochhaus, G., et al., 2016. Scope and relevance of a pulmonary biopharmaceutical classification system AAPS/FDA/USP Workshop March 16–17th, 2015 in Baltimore, MD. *AAPS Open* 2, 1. <https://doi.org/10.1186/s41120-015-0002-x>.
- Iglesias-Mejuto, A., García-González, C.A., 2022. 3D-printed, dual crosslinked and sterile aerogel scaffolds for bone tissue engineering. *Polymers* 14, 1211. <https://doi.org/10.3390/polym14061211>.
- Illanes-Bordomás, C., Landin, M., García-González, C.A., 2023. Aerogels as carriers for oral administration of drugs: an approach towards colonic delivery. *Pharmaceutics* 15, 2639. <https://doi.org/10.3390/pharmaceutics15112639>.
- Illanes-Bordomás, C., Landin, M., García-González, C.A., 2025. Novel core-shell aerogel formulation for drug delivery based on alginate and konjac glucomannan: rational design using artificial intelligence tools. *Polymers* 17, 1919. <https://doi.org/10.3390/polym17141919>.
- Izadi, Z., Rashidi, M., Derakhshankhah, H., Dolati, M., Ghanbari Kermanshahi, M., Adibi, H., et al., 2023. Curcumin-loaded porous particles functionalized with pH-responsive cell-penetrating peptide for colorectal cancer targeted drug delivery. *RSC Adv.* 13, 34587–34597. <https://doi.org/10.1039/D3RA06270H>.
- Jia, C., Chang, H., Liu, T., Zhao, Z., Lv, Q., Li, W., 2026. The fluidized bed coating strategy for developing curcumin solid dispersion pellets with enhanced solubility and stability. *J. Pharm. Innov.* 21, 86. <https://doi.org/10.1007/s12247-025-10307-x>.
- Ke, W.-R., Chang, R.Y.K., Chan, H.-K., 2022. Engineering the right formulation for enhanced drug delivery. *Adv. Drug Deliv. Rev.* 191, 114561. <https://doi.org/10.1016/j.addr.2022.114561>.
- Keil, C., Hajnal, A., Keitel, J., Kieserling, H., Rohn, S., Athamneh, T., et al., 2024. Agar aerogel powder particles for future life science applications: fabrication and investigations on swelling behavior and cell compatibility. *Polym. Bull.* 81, 9977–9993. <https://doi.org/10.1007/s00289-024-05188-y>.
- Khudeev, I.I., Lebedev, A.E., Mochalova, M.S., Menshutina, N.V., 2024. Modeling and techno-economic optimization of the supercritical drying of silica aerogels. *Dry Technol* 42, 812–835. <https://doi.org/10.1080/07373937.2024.2318439>.
- Kistler, S.S., 1931. Coherent expanded aerogels and jellies. *Nature* 127, 741. <https://doi.org/10.1038/127741a0>.
- Kumar Rajanna, S., Vinjamur, M., Mukhopadhyay, M., 2015. Mechanism for formation of Hollow and Granular Silica Aerogel Microspheres from rice husk ash for drug delivery. *J. Non Cryst. Solids* 429, 226–231. <https://doi.org/10.1016/j.jnoncrysol.2015.09.015>.
- Lázár, I., Celko, L., Menelaou, M., 2023. Aerogel-based materials in bone and cartilage tissue engineering—a review with future implications. *Gels* 9, 746. <https://doi.org/10.3390/gels9090746>.
- Kang, P., Lee, G., George, L., Gould, A., 2006. Aerogel powder therapeutic agents. *US6994842B2*, 2006.
- Lee, B.-B., Ravindra, P., Chan, E.-S., 2013. Size and shape of calcium alginate beads produced by extrusion dripping. *Chem. Eng. Technol.* 36, 1627–1642. <https://doi.org/10.1002/ceat.201300230>.
- Lefebvre, A.H., McDonnell, V.G., 2017. *Atomization and Sprays*, Second Edition. Taylor & Francis, CRC Press, Boca Raton, FL, USA. <https://doi.org/10.1201/9781315120911>.
- Chiesi Limited. *Fostair NEXThaler 200 micrograms/6 micrograms per actuation inhalation powder: Summary of Product Characteristics.* MedicinesOrgUk 2019. <https://www.medicines.org.uk/emc/product/5075/smpc> (accessed September 24, 2025).
- López-Iglesias, C., Barros, J., Ardao, I., Gurikov, P., Monteiro, F.J., Smirnova, I., et al., 2020. Jet cutting technique for the production of chitosan aerogel microparticles loaded with vancomycin. *Polymers* 12, 273. <https://doi.org/10.3390/polym12020273>.
- López-Iglesias, C., Barros, J., Ardao, I., Monteiro, F.J., Alvarez-Lorenzo, C., Gómez-Amoza, J.L., et al., 2019b. Vancomycin-loaded chitosan aerogel particles for chronic wound applications. *Carbohydr. Polym.* 204, 223–231. <https://doi.org/10.1016/j.carbpol.2018.10.012>.
- López-Iglesias, C., Casielles, A.M., Altay, A., Bettini, R., Alvarez-Lorenzo, C., García-González, C.A., 2019a. From the printer to the lungs: Inkjet-printed aerogel particles for pulmonary delivery. *Chem. Eng. J.* 357, 559–566. <https://doi.org/10.1016/j.cej.2018.09.159>.
- Lovskaya, D., Menshutina, N., Mochalova, M., Nosov, A., Grebenyuk, A., 2020. Chitosan-based aerogel particles as highly effective local hemostatic agents: production process and in vivo evaluations. *Polymers* 12, 2055. <https://doi.org/10.3390/polym12092055>.
- Mallepally, R.R., Bernard, I., Marin, M.A., Ward, K.R., McHugh, M.A., 2013. Superabsorbent alginate aerogels. *J. Supercrit. Fluids* 79, 202–208. <https://doi.org/10.1016/j.supflu.2012.11.024>.
- Manke, E., Rastar, B., Bueno, A., Schroeter, B., Smirnova, I., 2026. Continuous drying of alginate aerogel particles: Residence time measurement and process optimization under high pressure conditions. *J. Supercrit. Fluids* 231, 106888. <https://doi.org/10.1016/j.supflu.2026.106888>.
- Manzocco, L., Mikkonen, K.S., García-González, C.A., 2021. Aerogels as porous structures for food applications: Smart ingredients and novel packaging materials. *Food Struct.* 28, 100188. <https://doi.org/10.1016/j.foostr.2021.100188>.
- Mazurek, L., Kuś, M., Jurak, J., Rybka, M., Kuczeriszka, M., Stradczuk-Mazurek, M., et al., 2025. Biomedical potential of alginate wound dressings – From preclinical

- studies to clinical applications: a review. *Int. J. Biol. Macromol.* 309, 142908. <https://doi.org/10.1016/j.ijbiomac.2025.142908>.
- Menshutina, N.V., Lovskaya, D.D., Lebedev, A.E., Lebedev, E.A., 2017. Production of sodium alginate-based aerogel particles using supercritical drying in units with different volumes. *Russ. J. Phys. Chem. B* 11, 1296–1305. <https://doi.org/10.1134/S1990793117080073>.
- Menshutina, N.V., Uvarova, A.A., Mochalova, M.S., Lovskaya, D.D., Tsygankov, P.Y., Gurina, O.I., et al., 2023. Biopolymer aerogels as nasal drug delivery systems. *Russ. J. Phys. Chem. B* 17, 1507–1518. <https://doi.org/10.1134/S1990793123070163>.
- Mohammed, A.S.A., Naveed, M., Jost, N., 2021. Polysaccharides; classification, chemical properties, and future perspective applications in fields of pharmacology and biological medicine (a review of current applications and upcoming potentialities). *J. Polym. Environ.* 29, 2359–2371. <https://doi.org/10.1007/s10924-021-02052-2>.
- Morales, E., Quilaqueo, M., Morales-Medina, R., Drusch, S., Navia, R., Montillet, A., et al., 2024. Pectin–chitosan hydrogel beads for delivery of functional food ingredients. *Foods* 13, 2885. <https://doi.org/10.3390/foods13182885>.
- Munarin, F., Tanzi, M.C., Petrini, P., 2012. Advances in biomedical applications of pectin gels. *Int. J. Biol. Macromol.* 51, 681–689. <https://doi.org/10.1016/j.ijbiomac.2012.07.002>.
- Murillo-Cremaes, N., Subra-Paternault, P., Saurina, J., Roig, A., Domingo, C., 2014. Compressed antisolvent process for polymer coating of drug-loaded aerogel nanoparticles and study of the release behavior. *Colloid Polym. Sci.* 292, 2475–2484. <https://doi.org/10.1007/s00396-014-3260-6>.
- Omer, K., Ashgriz, N., 2011. *Spray Nozzles*. Sprays, Boston, MA, USA, pp. 497–579. [https://doi.org/10.1007/978-1-4419-7264-4\\_24](https://doi.org/10.1007/978-1-4419-7264-4_24).
- O'Sullivan, J.J., Norwood, E.-A., O'Mahony, J.A., Kelly, A.L., 2019. Atomisation technologies used in spray drying in the dairy industry: A review. *J. Food Eng.* 243, 57–69. <https://doi.org/10.1016/j.jfoodeng.2018.08.027>.
- Obaidat, R.M., Tashtoush, B.M., Bayan, M.F., Al Bustami, T.R., Alnaief, M., 2015. Drying using supercritical fluid technology as a potential method for preparation of chitosan aerogel microparticles. *AAPS PharmSciTech* 16, 1235–1244. <https://doi.org/10.1208/s12249-015-0312-2>.
- Obaidat, R.M., Alnaief, M., Mashaqbeh, H., 2018. Investigation of carrageenan aerogel microparticles as a potential drug carrier. *AAPS PharmSciTech* 19, 2226–2236. <https://doi.org/10.1208/s12249-018-1021-4>.
- Okkabaz, J.L., Darvishi, S., Akgün, İ.S., Barım, Ş.B., Özgünül, E., Kuduğ, D., et al., 2026. A new framework for 3D printing aerogels with additives: hardware and ink development. *ACS Omega* 11, 340–348. <https://doi.org/10.1021/acsomega.5c02676>.
- Owusu, S.Y., Amo-Boateng, M., Soni, R.U., 2025. Machine learning predictions of drug release from isocyanate-derived aerogels. *J. Mater. Chem. B* 13, 6233–6245. <https://doi.org/10.1039/D5TB00289C>.
- Ozemes Taylan, G., İllanes-Bordomás, C., Guven, O., Erkan, E., Erinsal, S.Ç., Oztop, M. H., et al., 2025. Core-shell aerogel design for enhanced oral insulin delivery. *Int. J. Pharm.* 669, 125038. <https://doi.org/10.1016/j.ijpharm.2024.125038>.
- Pantić, M., Horvat, G., Knez, Ž., Novak, Z., 2020. Preparation and characterization of chitosan-coated pectin aerogels: curcumin case study. *Molecules* 25, 1187. <https://doi.org/10.3390/molecules25051187>.
- Pantić, M., Kravanja, K.A., Knez, Ž., Novak, Z., 2021. Influence of the impregnation technique on the release of esomeprazole from various bioaerogels. *Polymers* 13, 1882. <https://doi.org/10.3390/polym13111882>.
- Payanda Konuk, O., Alshuhle, A.A.A.M., Yousefzadeh, H., Ulker, Z., Bozbag, S.E., García-González, C.A., et al., 2023. The effect of synthesis conditions and process parameters on aerogel properties. *Front. Chem.* 11, 1294520. <https://doi.org/10.3389/fchem.2023.1294520>.
- Pei, J., Palanisamy, C.P., Alugoju, P., Anthikapalli, N.V.A., Natarajan, P.M., Umapathy, V.R., et al., 2023. A comprehensive review on bio-based materials for chronic diabetic wounds. *Molecules* 28, 604. <https://doi.org/10.3390/molecules28020604>.
- Perrechil, F.A., Sato, A.C.K., Cunha, R.L., 2011.  $\kappa$ -Carrageenan–sodium caseinate microgel production by atomization: critical analysis of the experimental procedure. *J. Food Eng.* 104, 123–133. <https://doi.org/10.1016/j.jfoodeng.2010.12.004>.
- Plawsky, J.L., Littman, H., Paccione, J.D., 2010. Design, simulation, and performance of a draft tube spout fluid bed coating system for aerogel particles. *Powder Technol.* 199, 131–138. <https://doi.org/10.1016/j.powtec.2009.12.009>.
- Poncelat, D., Lencki, R., Beaulieu, C., Halle, J.P., Neufeld, R.J., Fourmier, A., 1992. Production of alginate beads by emulsification/internal gelation. I. Methodology. *Appl. Microbiol. Biotechnol.* 38. <https://doi.org/10.1007/BF00169416>.
- Poncelat, D., Neufeld, R., Bugarski, B., Amsden, B.G., Zhu, J., Goosen, M.F.A., 1994. A Parallel plate electrostatic droplet generator: Parameters affecting microbead size. *Appl. Microbiol. Biotechnol.* 42, 251–255. <https://doi.org/10.1007/bf00902725>.
- Poncelat, D., Babak, V.G., Neufeld, R.J., Goosen, M.F.A., Bugarski, B., 1999. Theory of electrostatic dispersion of polymer solutions in the production of microgel beads containing biocatalyst. *Adv. Colloid Interface Sci.* 79, 213–228. [https://doi.org/10.1016/S0001-8686\(97\)00037-7](https://doi.org/10.1016/S0001-8686(97)00037-7).
- Prausnitz, M.R., Mitragotri, S., Langer, R., 2004. Current status and future potential of transdermal drug delivery. *Nat. Rev. Drug Discov.* 3, 115–124. <https://doi.org/10.1038/nrd1304>.
- Prüsse, U., Bilancetti, L., Bučko, M., Bugarski, B., Bukowski, J., Gemeiner, P., et al., 2008. Comparison of different technologies for alginate beads production. *Chem. Pap.* 62. <https://doi.org/10.2478/s11696-008-0035-x>.
- Prübe, U., Fox, B., Kirchhoff, M., Bruske, F., Breford, J., Vorlop, K.-D., 1998. New process (jet cutting method) for the production of spherical beads from highly viscous polymer solutions. *Chem. Eng. Technol.* 21, 29–33. [https://doi.org/10.1002/\(sici\)1521-4125\(199801\)21:1%253C29:aid-ccat29%253E3.0.co;2-y](https://doi.org/10.1002/(sici)1521-4125(199801)21:1%253C29:aid-ccat29%253E3.0.co;2-y).
- Raman, S.P., Keil, C., Dieringer, P., Hübner, C., Bueno, A., Gurikov, P., et al., 2019. Alginate aerogels carrying calcium, zinc and silver cations for wound care: fabrication and metal detection. *J. Supercrit. Fluids* 153, 104545. <https://doi.org/10.1016/j.supflu.2019.104545>.
- Remuñán-Pose, P., López-Iglesias, C., Iglesias-Mejuto, A., Mano, J.F., García-González, C.A., Rial-Hermida, M.I., 2022. Preparation of vancomycin-loaded aerogels implementing inkjet printing and superhydrophobic surfaces. *Gels* 8, 417. <https://doi.org/10.3390/gels8070417>.
- Rodríguez-Dorado, R., Landín, M., Altai, A., Russo, P., Aquino, R.P., Del Gaudio, P., 2018. A novel method for the production of core-shell microparticles by inverse gelation optimized with artificial intelligent tools. *Int. J. Pharm.* 538, 97–104. <https://doi.org/10.1016/j.ijpharm.2018.01.023>.
- Rodríguez-Dorado, R., López-Iglesias, C., García-González, C.A., Auriemma, G., Aquino, R.P., Del Gaudio, P., 2019. Design of aerogels, cryogels and xerogels of alginate: effect of molecular weight, gelation conditions and drying method on particles' micromeritics. *Molecules* 24, 1049. <https://doi.org/10.3390/molecules24061049>.
- Rolison, D.R., Sassin, M.B., Long, J.W., 2023. Aerogels for Electrochemical Energy Storage Applications. In: Aegerter, M.A., Leventis, N., Koebel, M., Steiner III, S.A. (Eds.), *Springer Handb. Aerogels*. Springer International Publishing, Cham, Switzerland, pp. 1305–1332. [https://doi.org/10.1007/978-3-030-27322-4\\_50](https://doi.org/10.1007/978-3-030-27322-4_50).
- Rajasekar, P., Swetha P, Suwathi S, Rishikesavan S., 2025. 9 Biomaterials and surface modifications. In: Singh Y, Bansal G, editors. *Biotribology*, De Gruyter; 2025, p. 209–36. doi:10.1515/978311563176-009.
- Ruiz, F., Cavier, J.-Y. Method for continuous aerogel production. WO2018007740A1, 2018.
- Salawi, A., 2022. Pharmaceutical coating and its different approaches, a review. *Polymers* 14, 3318. <https://doi.org/10.3390/polym14163318>.
- Schroeter, B., Jung, I., Bauer, K., Gurikov, P., Smirnova, I., 2021b. Hydrophobic modification of biopolymer aerogels by cold plasma coating. *Polymers* 13, 3000. <https://doi.org/10.3390/polym13173000>.
- Schroeter, B., Jeansathawong, P., Hajnal, A., Gurikov, P., 2023. Wet milling of alginate alco- and hydrogel composites: a facile top-down approach for continuous production of aerogel microparticles. *Macromol. Mater. Eng.* 308, 2200674. <https://doi.org/10.1002/mame.202200674>.
- Schroeter, B., Yonkova, V.P., Goslinska, M., Orth, M., Pietsch, S., Gurikov, P., et al., 2021c. Spray coating of cellulose aerogel particles in a miniaturized spouted bed. *Cellul.* 28, 7795–7812. <https://doi.org/10.1007/s10570-021-04032-0>.
- Schroeter, B., Yonkova, V.P., Niemeyer, N.A.M., Jung, I., Preibisch, I., Gurikov, P., et al., 2021a. Cellulose aerogel particles: control of particle and textural properties in jet cutting process. *Cellul.* 28, 223–239. <https://doi.org/10.1007/s10570-020-03555-2>.
- Schwan, M., Schettler, J., Badaczewski, F.M., Heinrich, C., Smarsly, B.M., Milow, B., 2020. The effect of pulverization methods on the microstructure of stiff, ductile, and flexible carbon aerogels. *J. Mater. Sci.* 55, 5861–5879. <https://doi.org/10.1007/s10853-020-04397-w>.
- Scoutaris, N., Ross, S., Douroumis, D., 2016. Current trends on medical and pharmaceutical applications of inkjet printing technology. *Pharm. Res.* 33, 1799–1816. <https://doi.org/10.1007/s11095-016-1931-3>.
- Sécher, T., Bodier-Montagutelli, E., Guillon, A., Heuzé-Vourc'h, N., 2020. Correlation and clinical relevance of animal models for inhaled pharmaceuticals and biopharmaceuticals. *Adv. Drug Deliv. Rev.* 167, 148–169. <https://doi.org/10.1016/j.addr.2020.06.029>.
- Sellitto, M.R., Amante, C., Aquino, R.P., Russo, P., Rodríguez-Dorado, R., Neagu, M., et al., 2023. Hollow particles obtained by prilling and supercritical drying as a potential conformable dressing for chronic wounds. *Gels* 9, 492. <https://doi.org/10.3390/gels9060492>.
- Shi, W., Ching, Y.C., Chuah, C.H., 2021. Preparation of aerogel beads and microspheres based on chitosan and cellulose for drug delivery: A review. *Int. J. Biol. Macromol.* 170, 751–767. <https://doi.org/10.1016/j.ijbiomac.2020.12.214>.
- Smirnova, I., Suttiruengwong, S., Aerogels, A.W., 2005. Tailor-made carriers for immediate and prolonged drug release. *KONA Powder. Part J* 23 (86–97). <https://doi.org/10.14356/kona.2005012>.
- Song, Y., Fang, R., Liu, N., Wang, T., Zhou, T., Zhang, M., et al., 2025. A comparative study on the coating performance of Wurster, bottom and top spray fluidized bed coaters. *Chem. Eng. Res. Des.* 220, 1–15. <https://doi.org/10.1016/j.cherd.2025.06.028>.
- Tiryaki, E., Başaran Elalmış, Y., Karakuzu İklizler, B., Yücel, S., 2020. Novel organic/inorganic hybrid nanoparticles as enzyme-triggered drug delivery systems: dextran and dextran aldehyde coated silica aerogels. *J. Drug. Deliv. Sci. Technol.* 56, 101517. <https://doi.org/10.1016/j.jddst.2020.101517>.
- Tkalec, G., Knez, Ž., Novak, Z., 2016. pH sensitive mesoporous materials for immediate or controlled release of NSAID. *Microporous Mesoporous Mater.* 224, 190–200. <https://doi.org/10.1016/j.micromeso.2015.11.048>.
- Tyagi, M., Barman, B., 2026. Synthesis of Thin Films. In: Sharma, S., Raj, V.B. (Eds.), *Properties and Applications of Advanced Materials*, 1st ed. Wiley, pp. 169–202. <https://doi.org/10.1002/9783527854165.ch8>.
- Ulker, Z., Erkey, C., 2014. An emerging platform for drug delivery: Aerogel based systems. *J. Control. Release* 177, 51–63. <https://doi.org/10.1016/j.jconrel.2013.12.033>.
- Ulker, Z., Erkey, C., 2014. A novel hybrid material: An inorganic silica aerogel core encapsulated with a tunable organic alginate aerogel layer. *RSC Adv.* 4, 62362–62366. <https://doi.org/10.1039/C4RA09089F>.
- Valente, S.A., Silva, L.M., Lopes, G.R., Sarmiento, B., Coimbra, M.A., Passos, C.P., 2022. Polysaccharide-based formulations as potential carriers for pulmonary delivery – A review of their properties and fates. *Carbohydr. Polym.* 277, 118784. <https://doi.org/10.1016/j.carbpol.2021.118784>.

- Vareda, J.P., García-González, C.A., Valente, A.J.M., Simón-Vázquez, R., Stipetic, M., Durães, L., 2021. Insights on toxicity, safe handling and disposal of silica aerogels and amorphous nanoparticles. *Environ. Sci. Nano* 8, 1177–1195. <https://doi.org/10.1039/D1EN00026H>.
- Verma, S., Sharma, P.K., Malviya, R., Das, S., 2024. Advances in aerogels formulations for pulmonary targeted delivery of therapeutic agents: safety, efficacy and regulatory aspects. *Curr. Pharm. Biotechnol.* 25, 1939–1951. <https://doi.org/10.2174/0113892010275613231120031855>.
- Veronovski, A., Knez, Ž., Novak, Z., 2013. Preparation of multi-membrane alginate aerogels used for drug delivery. *J. Supercrit. Fluids* 79, 209–215. <https://doi.org/10.1016/j.supflu.2013.01.025>.
- Wang, L., You, D.-S., Guo, D., Zhuang, X.-C., Yuan, T., Qiu, D., 2025. Preparation and properties of sodium carboxymethyl cellulose microspheres by dropping method. *ACS Omega* 10, 4754–4762. <https://doi.org/10.1021/acsomega.4c09736>.
- Wanning, S., Süverkrüp, R., Lamprecht, A., 2015. Pharmaceutical spray freeze drying. *Int. J. Pharm.* 488, 136–153. <https://doi.org/10.1016/j.ijpharm.2015.04.053>.
- Whelehan, M., Marison, I.W., 2011. Microencapsulation using vibrating technology. *J. Microencapsul.* 28, 669–688. <https://doi.org/10.3109/02652048.2011.586068>.
- Workamp, M., Alaie, S., Dijkman, J.A., 2016. Coaxial air flow device for the production of millimeter-sized spherical hydrogel particles. *Rev. Sci. Instrum.* 87, 125113. <https://doi.org/10.1063/1.4972587>.
- Xiang, Y., Yan, M., Li, L., Xiao, Y., Sun, H., Zhang, Z., et al., 2025. Low thermal conductivity and self-cleaning silica aerogel coating based on a secondary coating encapsulation strategy. *Constr. Build. Mater.* 472, 140878. <https://doi.org/10.1016/j.conbuildmat.2025.140878>.
- Yousefzadeh, H., Akgün, I.S., Barim, S.B., Sari, T.B., Eris, G., Uzunlar, E., et al., 2022. Supercritical fluid reactive deposition: A process intensification technique for synthesis of nanostructured materials. *Chem. Eng. Process. – Process., Intensif.* 176, 108934. <https://doi.org/10.1016/j.cep.2022.108934>.
- Zafar, S., Sayed, E., Rana, S.J., Rasekh, M., Onaiwu, E., Nazari, K., et al., 2024. Particulate atomisation design methods for the development and engineering of advanced drug delivery systems: A review. *Int. J. Pharm.* 666, 124771. <https://doi.org/10.1016/j.ijpharm.2024.124771>.
- Zemke, F., Scoppola, E., Simon, U., Bekheet, M.F., Wagermaier, W., Gurlo, A., 2022. Springback effect and structural features during the drying of silica aerogels tracked by in-situ synchrotron X-ray scattering. *Sci. Rep.* 12, 7537. <https://doi.org/10.1038/s41598-022-11127-6>.
- Zhai, T., Zheng, Q., Cai, Z., Xia, H., Gong, S., 2016. Synthesis of polyvinyl alcohol/cellulose nanofibril hybrid aerogel microspheres and their use as oil/solvent superabsorbents. *Carbohydr. Polym.* 148, 300–308. <https://doi.org/10.1016/j.carbpol.2016.04.065>.
- Zhang, S., Li, R., Jiang, T., Gao, Y., Zhong, K., Cheng, H., et al., 2024. Inhalable nanomedicine for lung cancer treatment. *Smart Mater. Med.* 5, 261–280. <https://doi.org/10.1016/j.smaim.2024.04.001>.
- Zhang, M., Lu, H., Xie, L., Liu, X., Cun, D., Yang, M., 2023. Inhaled RNA drugs to treat lung diseases: disease-related cells and nano–bio interactions. *Adv. Drug Deliv. Rev.* 203, 115144. <https://doi.org/10.1016/j.addr.2023.115144>.
- Zhou, H., Tu, Q.Y., Wang, H.G., 2019. Investigation of the complex gas-solids flow characteristics in a fluidized bed with a Wurster tube by process tomography and CFD simulation. *Powder Technol.* 357, 117–133. <https://doi.org/10.1016/j.powtec.2019.08.099>.